Dephasing in quantum chaotic transport: A semiclassical approach

Robert S. Whitney,[1] Philippe Jacquod,[2] and Cyril Petitjean[3,4]
[1]*Institut Laue-Langevin, 6 rue Jules Horowitz, Boîte Postale 156, 38042 Grenoble, France*
[2]*Physics Department, University of Arizona, 1118 East 4th Street, Tucson, Arizona 85721, USA*
[3]*Département de Physique Théorique, Université de Genève, CH-1211 Genève 4, Switzerland*
[4]*Institut I-Theoretische Physik, Universität Regensburg, Universitätsstrasse 31, D-93040 Regensburg, Germany*
(Received 7 September 2007; published 15 January 2008)

We investigate the effect of dephasing (decoherence) on quantum transport through open chaotic ballistic conductors in the semiclassical limit of small Fermi wavelength to system size ratio, $\lambda_F/L \ll 1$. We use the trajectory-based semiclassical theory to study a two-terminal chaotic dot with decoherence originating from (i) an external closed quantum chaotic environment, (ii) a classical source of noise, and (iii) a voltage probe, i.e., an additional current-conserving terminal. We focus on the pure dephasing regime, where the coupling to the external source of dephasing is so weak that it does not induce energy relaxation. In addition to the universal algebraic suppression of weak localization, we find an exponential suppression of weak localization $\propto \exp[-\tilde{\tau}/\tau_\phi]$, with the dephasing rate τ_ϕ^{-1}. The parameter $\tilde{\tau}$ depends strongly on the source of dephasing. For a voltage probe, $\tilde{\tau}$ is of order the Ehrenfest time $\propto \ln[L/\lambda_F]$. In contrast, for a chaotic environment or a classical source of noise, it has the correlation length ξ of the coupling or noise potential replacing the Fermi wavelength λ_F. We explicitly show that the Fano factor for shot noise is unaffected by decoherence. We connect these results to earlier works on dephasing due to electron-electron interactions and numerically confirm our findings.

DOI: 10.1103/PhysRevB.77.045315 PACS number(s): 05.45.Mt, 03.65.Yz, 73.23.−b, 74.40.+k

I. INTRODUCTION

A. Dephasing in the universal regime

Electronic systems in the mesoscopic regime are ideal testing grounds for investigating the quantum-to-classical transition from a microscopic coherent world (where quantum interference effects prevail) to a macroscopic classical world.[1] On one hand, their size is intermediate between macroscopic and microscopic (atomic) systems; on the other hand, today's experimental control over their design and precision of measurement allows one to investigate them in regimes ranging from almost fully coherent to purely classical.[2–4] The extent to which quantum coherence is preserved in these systems is usually determined by the ratio $\tau_\phi/\tau_{\rm cl}$ of the dephasing time τ_ϕ to some relevant classical time scale $\tau_{\rm cl}$. For instance, $\tau_{\rm cl}$ can be the traversal time through one arm of a two-path interferometer[5–7] or the average dwell time spent inside a quantum dot.[8–12] In a given experimental setup, τ_ϕ can often be tuned from $\tau_\phi > \tau_{\rm cl}$ (quantum coherent regime) to $\tau_\phi \ll \tau_{\rm cl}$ (purely classical regime) by varying externally applied voltages or the temperature of the sample.

Coherent effects abound in mesoscopic physics, the most important of them being the weak localization, universal conductance fluctuations, and Aharonov-Bohm interferences in transport, as well as persistent currents.[2–4] The disappearance of these effects as dephasing processes are turned on has raised a lot of theoretical[8–25] and experimental[26–33] interest. Focusing on transport through ballistic systems, dephasing is usually investigated using mostly phenomenological models of dephasing,[16–21] the most successful of which are the voltage-probe and dephasing-lead models.[16,17] In these models, a cavity is connected to two external, left (L) and right (R), transport leads, carrying N_R and N_L transport channels, respectively. Dephasing is modeled by connecting a third "fictitious" lead to the system, with a voltage set such that no current flows through it on average. Electrons leaving the system through this third lead are thus reinjected at some later time, with a randomized phase (and randomized momentum). These models of dephasing present the significant advantage that the standard scattering approach to transport can be applied as in fully coherent systems, once it is properly extended to account for the presence of the third lead.

Using random matrix theory (RMT), the voltage- and dephasing-probe models[34] predict an algebraic suppression of the weak-localization contribution to the conductance (in units of $2e^2/h$),[35]

$$g_{\rm RMT}^{\rm wl} = -\frac{N_R N_L}{[N_R+N_L]^2}[1+\tau_D/\tau_\phi]^{-1}, \tag{1}$$

where $-N_R N_L/[N_R+N_L]^2$ is the weak-localization correction in the absence of dephasing. Similarly, universal conductance fluctuations become[11]

$$\delta g_{\rm RMT}^2 = \frac{2}{\beta}\frac{N_R^2 N_L^2}{[N_R+N_L]^4}[1+\tau_D/\tau_\phi]^{-2} \tag{2}$$

and are thus damped below their value $(2/\beta)N_R^2N_L^2/[N_R+N_L]^2$ (in units of $4e^4/h^2$) for fully coherent systems with ($\beta=1$) or without ($\beta=2$) time-reversal symmetry. For a fictitious lead connected to a two-dimensional cavity (a lateral quantum dot) via a point contact of transparency ρ and carrying N_3 channels, one has $\tau_\phi = mA/\hbar\rho N_3$, with the electron mass m and the area A of the cavity. Similarly, the dwell time through the cavity is given by $\tau_D = mA/\hbar(N_{\rm L}+N_{\rm R})$.

The dephasing- and voltage-probe models account for dephasing at the phenomenological level only, without reference to the microscopic processes leading to dephasing. At

sufficiently low temperature, it is accepted that the dephasing arises dominantly from electronic interactions, which, in diffusive systems, can be well modeled by a classical-noise potential.[8,9] Remarkably enough, this approach reproduces the RMT results of Eqs. (1) and (2) with τ_ϕ set by the noise power. These results are moreover quite robust in diffusive systems. They are essentially insensitive to most noise-spectrum details and hold for various sources of noise such as electron-electron and electron-phonon interactions, or external microwave fields. For this reason, it is often assumed that dephasing is system independent and exhibits a character of universality well described by the RMT of transport applied to the dephasing- and voltage-probe models.[35]

B. Departure from random matrix theory universality

According to the Bohigas-Giannoni-Schmit surmise,[36] closed chaotic systems exhibit statistical properties of Hermitian RMT[37] in the short wavelength limit. Opening up the system, transport properties derive from the corresponding scattering matrix, which is determined by both the Hamiltonian of the closed system and its coupling to external leads.[38] It has been shown that for not too strong coupling, and when the Hamiltonian matrix of the closed system belongs to one of the Gaussian ensembles of random Hermitian matrices, the corresponding scattering matrix is an element of one of the circular ensembles of unitary random matrices.[39] One thus expects that, in the semiclassical limit of large ratio L/λ_F of the system size to Fermi wavelength, transport properties of quantum chaotic ballistic systems are well described by the RMT of transport. This surmise has recently been verified semiclassically.[40]

The regime of validity of RMT is generally bounded by the existence of finite time scales, however, and it was noticed by Aleiner and Larkin that, while the dephasing time τ_ϕ gives the long time cutoff for quantum interferences, an *Ehrenfest time* scale appears in the quantum chaotic system in the deep semiclassical limit, which determines the short-time onset of these interferences.[14] The Ehrenfest time τ_E corresponds to the time it takes for the underlying chaotic classical dynamics to stretch an initially localized wave packet to a macroscopic, classical length scale. In open cavities, the latter can be either the system size L or the width W of the opening to the leads. Accordingly, one can define the closed cavity, $\tau_E^{\rm cl}=\lambda^{-1}\ln[L/\lambda_F]$, and the open cavity Ehrenfest time, $\tau_E^{\rm op}=\lambda^{-1}\ln[W^2/\lambda_F L]$.[41,42] The emergence of a finite τ_E strongly affects quantum effects in transport, and recent analytical and numerical investigations of quantum chaotic systems have shown that weak localization[14,43–46] and shot noise[47–50] are exponentially suppressed $\propto\exp[-\tau_E/\tau_D]$ in the absence of dephasing ($\tau_\phi\to\infty$). Interestingly enough, the deep semiclassical limit of finite τ_E sees the emergence of a quantitatively dissimilar behavior of weak localization and quantum parametric conductance fluctuations, the latter exhibiting no τ_E dependence in the absence of dephasing.[51–54] These results are not captured by RMT; instead, one has to rely on quasiclassical approaches[14,44] or semiclassical methods[43,45,46,55,56] to derive them.

C. Dephasing in the deep semiclassical limit

The behavior of quantum corrections to transport at finite τ_E in the presence of dephasing was briefly investigated analytically in Ref. 14, for a model of classical noise with large angle scattering, and numerically in Ref. 23, for the dephasing-lead model with a tunnel barrier. Intriguingly enough, the two approaches delivered the same result that quantum effects are exponentially suppressed $\propto\exp[-\tau_E/\tau_\phi]$. This suggested that dephasing retains a character of universality even in the deep semiclassical limit. More recent investigations have, however, showed that at finite Ehrenfest time, Eq. (1) becomes[25] (see also Ref. 24)

$$g^{\rm wl}=-\frac{N_R N_L}{[N_R+N_L]^2}\frac{\exp[-(\tau_E^{\rm cl}/\tau_D+\tilde{\tau}/\tau_\phi)]}{1+\tau_D/\tau_\phi}, \tag{3}$$

with a strongly system-dependent time scale $\tilde{\tau}$. Reference 25 showed that, for the dephasing-lead model, $\tilde{\tau}=\tau_E^{\rm cl}+(1-\rho)\tau_E^{\rm op}$ in terms of the transparency ρ of the contacts to the leads, which provides theoretical understanding for the numerical findings of Ref. 23. If, however, one considers a system-environment model, where the environment is mimicked by electrons in a nearby closed quantum chaotic dot, one has $\tilde{\tau}=\tau_\xi$, where

$$\tau_\xi=\lambda^{-1}\ln[(L/\xi)^2], \tag{4}$$

in terms of the correlation length ξ of the interdot interaction potential.

On the experimental front, an exponential suppression $\propto\exp[-T/T_c]$ of weak localization with temperature has been reported in Ref. 29. Taking $\tau_\phi\sim T^{-1}$ as for dephasing by electronic interactions in two-dimensional diffusive systems, this result was interpreted as the first experimental confirmation of Eq. (3). There is no other theory for such an exponential behavior of weak localization; however, the temperature range over which this experiment has been performed makes it unclear whether the ballistic,[13,15] $\tau_\phi\sim T^{-2}$, or the diffusive dephasing time determines the Ehrenfest time dependence of dephasing (see the discussion in Ref. 24) .

D. Outline of this paper

In the present paper, we amplify on Ref. 25 and extend the analytical derivation of Eq. (3) briefly presented there. We investigate three different models of dephasing and show that the suppression of weak-localization corrections to the conductance is strongly model dependent. First, we consider an external environment modeled by a capacitively coupled, closed quantum dot. We restrict ourselves to the regime of pure dephasing, where the environment does not alter the classical dynamics of the system. Second, we discuss dephasing by a classical-noise field. Third, following Ref. 56, we provide a semiclassical treatment of transport in the dephasing-lead model. For these three models, we reproduce Eq. (3) and derive the exact dependence of $\tilde{\tau}$ on microscopic details of the models considered. All our results are summarized in Table I.

The outline of this paper is as follows. In Sec. II, we present the treatment of the system-environment model, focusing, in particular, on the construction of a scattering approach to transport that incorporates the coupling to external degrees of freedom. We apply this formalism to a model of

TABLE I. Summary of the known results to date on the nature of the exponential term $\exp[-\tilde{\tau}/\tau_\phi]$ in the dephasing [cf. Eq. (3)]. Results that are not referenced are obtained in the present paper and in Ref. 25. Here, we list the value of $\tilde{\tau}$ for different transport quantities and different sources of dephasing, all in the pure dephasing regime (the phase-breaking regime of Ref. 17). The parameter ξ differs slightly from system to system (see text for details); however, it is always related to the correlation length of the interaction with the environment. The results of Ref. 24 neglect τ_ξ contributions (so "0" could indicate a $\tilde{\tau}$ of order τ_ξ); they are also only valid for $\tau_E^{cl} \gg \tau_\phi$.

	Weak localization	Conductance fluctuations	Shot noise
System with environment	$\tilde{\tau}=\tau_\xi$	—	No dephasing
Classical noise (microwave, etc.)	$\tilde{\tau}=\tau_\xi$	$\tilde{\tau}\sim 0$, Ref. 24	No dephasing
e-e interactions within system	$\tilde{\tau}=\tau_E^{\mathrm{cl}}+\frac{1}{2}\tau_\xi$	$\tilde{\tau}\sim \frac{1}{2}\tau_E^{\mathrm{cl}}$, Ref. 24	No dephasing
System-gate e-e interactions	$\tilde{\tau}=\tau_\xi$	$\tilde{\tau}\sim \frac{1}{2}\tau_\xi$, follows from Ref. 24	No dephasing
Dephasing lead:			
No tunnel barrier	$\tilde{\tau}=\tau_E^{\mathrm{cl}}$	$\tilde{\tau}=0$	No dephasing, Ref. 57
Low transparency barrier	$\tilde{\tau}=\tau_E^{\mathrm{op}}+\tau_E^{\mathrm{cl}}\sim 2\tau_E^{\mathrm{cl}}$	$\tilde{\tau}\sim 2\tau_E^{\mathrm{cl}}$ (numerics), Ref. 23	No dephasing, Ref. 57

an open quantum dot coupled to a second, closed quantum dot. We present a detailed calculation of the Drude conductance and the weak-localization correction, including coherent backscattering, which explicitly preserves the unitarity of the S-matrix, and hence current conservation. This calculation is completed by a derivation of the Fano factor, showing that, in the pure dephasing limit, shot noise is insensitive to dephasing to leading order. In Sec. III, we present a model of dephasing via a classical-noise field (such as microwave noise). We consider classical Johnson-Nyquist noise models of dephasing due to electron-electron interactions within the system and dephasing due to charge fluctuations on nearby gates. In Sec. IV, we present a trajectory-based semiclassical calculation of conductance in the dephasing-lead model, both for fully transparent barriers and tunnel barriers. We also comment on dephasing in multiprobe configurations. Finally, Sec. V is devoted to numerical simulations confirming our analytical results. Summary and conclusions are presented in Sec. VI, while technical details are presented in the Appendix.

II. TRANSPORT THEORY FOR A SYSTEM WITH ENVIRONMENT

In the scattering approach to transport, the system is assumed fully coherent and all dissipative processes occur in the leads.[58] Apart from its coupling to the leads, the system is isolated. Here, we extend this formalism to include coupling to external degrees of freedom in the spirit of the standard theory of decoherence. The coupling to an environment can induce dephasing and relaxation. Here, we restrict ourselves to pure dephasing, where the system-environment coupling does not induce energy nor momentum relaxation in the system. In semiclassical language, we assume that classical trajectories supporting the electron dynamics are not modified by this coupling.

The starting point of the standard theory of decoherence is the total density matrix η_{tot} that includes both system and environmental degrees of freedom.[1] The observed properties of the system alone are contained in the reduced density matrix η_{sys}, obtained from η_{tot} by tracing over the environmental degrees of freedom. This procedure is probability conserving, $\mathrm{Tr}[\eta_{\mathrm{sys}}]=1$, but it renders the time evolution of η_{sys} nonunitary and, in particular, the off-diagonal elements of η_{sys} decay with time. This can be quantified by the basis independent purity,[59] $0 \leqslant \mathrm{Tr}[\eta_{\mathrm{sys}}^2] \leqslant 1$, which remains equal to 1 only in the absence of environment. We generalize this standard approach to the transport problem.

A. Scattering formalism in the presence of an environment

We consider two capacitively coupled chaotic cavities, as sketched in Fig. 1. The first one is the system (sys), an open, two-dimensional quantum dot, ideally connected to two external leads. The second one is a closed quantum dot, which

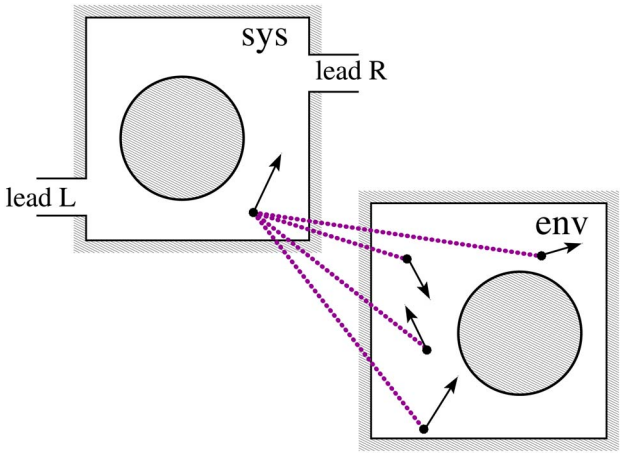

FIG. 1. (Color online) Schematic of the system-environment model. The system is an open quantum dot that is coupled to an environment in the shape of a second, closed dot.

plays the role of an environment (env). The two dots are capacitively coupled and, in particular, they do not exchange particles. Thus, current through the system is conserved. We require that the size of the contacts between the open system and the leads is much smaller than the perimeter of the system cavity but is still semiclassically large, so that the number of transport channels satisfies $1 \ll N_{L,R} \ll L/\lambda_F$. This ensures that the chaotic dynamics inside the dot has enough time to develop, $\lambda \tau_D \gg 1$, with the classical Lyapunov exponent λ. Electrons in the leads do not interact with the second dot. Few-electron double-dot systems have recently been the focus of intense experimental efforts.[60] Parallel geometries, of direct relevance to the present work, have been investigated in Refs. 61 and 62.

The total system is described by the following Hamiltonian:

$$\mathcal{H} = H_{\rm sys} + H_{\rm env} + \mathcal{U}. \tag{5}$$

Inside each cavity, the chaotic dynamics is generated by the corresponding one-particle Hamiltonian $H_{\rm sys,env}$. We only specify that the capacitive coupling potential $\mathcal{U}$ is a smooth function of the distance between the particles. It is characterized by its magnitude U and its correlation length ξ such that its typical gradient is U/ξ. Physically, ξ is determined by the electrostatic environment of the system, such as electric charges on the gates defining the dots and the amount of depletion of the electrostatic confinement potential between the gates and the inversion layer in semiconductor heterostructures. Generally speaking, U and ξ are independent parameters and can have different values in different systems and might even be tuned by applying external backgate voltages on a given system.

In the standard scattering approach, the transport properties of the system derive from its $(N_L+N_R)\times(N_L+N_R)$ scattering matrix[16]

$$\hat{\mathbf{S}} = \begin{pmatrix} \mathbf{s}_{LL} & \mathbf{s}_{RL} \\ \mathbf{s}_{LR} & \mathbf{s}_{RR} \end{pmatrix}, \tag{6}$$

which we write in terms of transmission ($\mathbf{t}=\mathbf{s}_{LR}$) and reflection ($\mathbf{r}=\mathbf{s}_{\alpha,\alpha}$, $\alpha \in \{L,R\}$) matrices. From $\hat{\mathbf{S}}$, the system's dimensionless conductance (conductance in units of $2e^2/h$) is given by

$$g = {\rm Tr}(\mathbf{t}^\dagger \mathbf{t}). \tag{7}$$

To include coupling to an environment in the scattering approach, we need to define an extended scattering matrix $\mathbb{S}$ that includes the external degrees of freedom. This is formally done in the Appendix, and our starting point is Eq. (A11) for the case of an initial product density matrix $\eta_{\rm tot} = \eta_{\rm sys}^{(n)} \otimes \eta_{\rm env}$, with $\eta_{\rm sys}^{(n)} = |n\rangle\langle n|$, $n \in \{1,\ldots,N_L\}$, and $\eta_{\rm env}$ the initial density matrix of the environment. We define the conductance matrix

$$g_{nm}^{(r)} = \langle m|{\rm Tr}_{\rm env}(\mathbb{S}[\eta_{\rm sys}^{(n)} \otimes \eta_{\rm env}]\mathbb{S}^\dagger)|m\rangle, \tag{8}$$

where ${\rm Tr}_{\rm env}$ stands for the trace over the environmental degrees of freedom. From this matrix, the dimensionless conductance is then given by

$$g = \sum_{n=0}^{N_R} \sum_{m=0}^{N_L} g_{nm}^{(r)}, \tag{9}$$

and Eq. (A11) reads

$$g = \sum_{n\in R; m\in L} \int d\mathbf{q} d\mathbf{q}_0 d\mathbf{q}_0' \langle \mathbf{q}_0|\eta_{\rm env}|\mathbf{q}_0'\rangle \mathbb{S}_{mn}(\mathbf{q},\mathbf{q}_0)[\mathbb{S}_{nm}(\mathbf{q},\mathbf{q}_0')]^*. \tag{10}$$

Equation (10) is the generalization of the Laudauer-Büttiker formula in the presence of an external environment. It constitutes the backbone of our trajectory-based semiclassical theory of dephasing.

B. Drude conductance

The semiclassical derivation of the one-particle scattering matrix has become standard.[63–65] Once we introduce the environment, we deal with a bipartite problem; here, we use the two-particle semiclassical propagator developed in the framework of entanglement and decoherence.[66,67] The extended scattering matrix elements can be written as

$$\mathbb{S}_{\rm mn}(\mathbf{q},\mathbf{q}_0) = -i\int_0^\infty dt \int_L dy_0 \int_R dy \frac{\langle m|y\rangle\langle y_0|n\rangle}{(2\pi\hbar)^{(d_{\rm sys}-1)/2}} \times \sum_{\gamma,\Gamma} \frac{A_\gamma A_\Gamma}{(2\pi\hbar)^{Nd/2}} e^{i(S_\gamma + S_\Gamma + \mathcal{S}_{\gamma,\Gamma})/\hbar}, \tag{11}$$

where we take a $d_{\rm sys}$-dimensional, one-particle system (throughout what follows, we take $d_{\rm sys}=2$), and a d-dimensional, N-particle environment. At this point, $\mathbb{S}$ depends on the coordinates of the environment and is given by a sum over pairs of classical trajectories, labeled γ for the system and Γ for the environment. The classical paths γ and Γ connect y_0 (on a cross section of lead L) and $\mathbf{q}_0$ (anywhere in the volume occupied by the environment) to y (on a cross section of lead R) and $\mathbf{q}$ (anywhere in the volume occupied by the environment) in the time $t=t_\gamma=t_\Gamma$. For an environment of N particles in d dimensions, $\mathbf{q}$ is an Nd component vector. In the regime of pure dephasing, these paths are solely determined by $H_{\rm sys}$ and $H_{\rm env}$. Each pair of paths gives a contribution weighted by the square root $A_\gamma A_\Gamma$ of the inverse determinant of the stability matrix[68,69] and oscillating with one-particle (S_γ and S_Γ, which include Maslov indices) and two-particle ($\mathcal{S}_{\gamma,\Gamma} = \int_0^t d\tau \mathcal{U}[\mathbf{y}_\gamma(\tau), \mathbf{q}_\Gamma(\tau)]$) action integrals accumulated along γ and Γ.

We insert Eq. (11) into Eq. (10), sum over channel indices with the semiclassical approximation[45,56] $\Sigma_n^{N_L} \langle y_0|n\rangle\langle n|y_0'\rangle \approx \delta(y_0'-y_0)$. For the environment, we make the random matrix ansatz that $\overline{\langle \mathbf{q}_0|\eta_{\rm env}|\mathbf{q}_0'\rangle} \approx (2\pi\hbar)^{Nd}\Xi_{\rm env}^{-1}\delta(\mathbf{q}_0'-\mathbf{q}_0)$, where $\Xi_{\rm env}$ is the environment phase-space volume. The dimensionless conductance then reads

$$g = \frac{(2\pi\hbar)^{-1}}{\Xi_{\rm env}} \int_0^\infty dt dt' \int_{\rm env} d\mathbf{q}_0 d\mathbf{q} \int_L dy_0 \int_R dy \times \sum_{\gamma,\Gamma;\gamma',\Gamma'} A_\gamma A_\Gamma A_{\gamma'} A_{\Gamma'} e^{i(\Phi_{\rm sys}+\Phi_{\rm env}+\Phi_{\mathcal{U}})}. \quad (12)$$

This is a quadruple sum over classical paths of the system (γ and γ', going from y_0 to y) and the environment (Γ and Γ', going from $\mathbf{q}_0$ to $\mathbf{q}$) with action phases

$$\Phi_{\rm sys} = [S_\gamma(y,y_0;t) - S_{\gamma'}(y,y_0;t')]/\hbar, \quad (13a)$$

$$\Phi_{\rm env} = [S_\Gamma(\mathbf{q},\mathbf{q}_0;t) - S_{\Gamma'}(\mathbf{q},\mathbf{q}_0;t')]/\hbar, \quad (13b)$$

$$\Phi_{\mathcal{U}} = [\mathcal{S}_{\gamma,\Gamma}(y,y_0;\mathbf{q},\mathbf{q}_0;t) - \mathcal{S}_{\gamma',\Gamma'}(y,y_0;\mathbf{q},\mathbf{q}_0;t')]/\hbar. \quad (13c)$$

We are interested in quantities averaged over variations in the energy or cavity shapes. For most sets of paths, the phase of a given contribution will oscillate wildly with these variations, so the contribution averages to zero. In the semiclassical limit, Eq. (12) is thus dominated by terms which satisfy a stationary phase condition (SPC), i.e., where the variation of $\Phi_{\rm sys}+\Phi_{\rm env}+\Phi_{\mathcal{U}}$ has to be minimized. In the regime of pure dephasing, individual variations of $\Phi_{\rm sys}$, $\Phi_{\rm env}$, and $\Phi_{\mathcal{U}}$ are uncorrelated. They are moreover dominated by variations of $\Phi_{\rm sys}$ and $\Phi_{\rm env}$, on which we therefore enforce two independent SPC's.

The dominant contributions that survive averaging are the diagonal ones. They give the Drude conductance. Indeed, setting $\gamma=\gamma'$ and $\Gamma=\Gamma'$ straightforwardly satisfies SPC's over $\Phi_{\rm sys}$ and $\Phi_{\rm env}$. These two SPC's require $t=t'$ and lead to an exact cancellation of all the phases $\Phi_{\rm sys}=\Phi_{\rm env}=\Phi_{\mathcal{U}}=0$. The dimensionless Drude conductance is given by

$$g^D = \int_0^\infty dt \int_{\rm env} d\mathbf{q}_0 d\mathbf{q} \int_L dy_0 \int_R dy \sum_{\gamma,\Gamma} \frac{A_\gamma^2 A_\Gamma^2}{(2\pi\hbar)\Xi_{\rm env}}. \quad (14)$$

From here on, the calculation proceeds along the lines of Ref. 45. The main idea is to relate semiclassical amplitudes with classical probabilities. This is done by the introduction of two sum rules that express the ergodic properties of open cavities, Eq. (15a), and of closed ones, Eq. (15b),

$$\sum_\gamma A_\gamma^2 [\cdots]_\gamma = \int_{-\pi/2}^{\pi/2} d\theta_0 d\theta P_{\rm sys}(\mathbf{Y},\mathbf{Y}_0;t)[\cdots]_{\mathbf{Y}_0}, \quad (15a)$$

$$\sum_\Gamma A_\Gamma^2 [\cdots]_\Gamma = \int d\mathbf{p}_0 d\mathbf{p} \tilde{P}_{\rm env}(\mathbf{Q},\mathbf{Q}_0;t)[\cdots]_{\mathbf{Q}_0}. \quad (15b)$$

Here, $P_{\rm sys}(\mathbf{Y},\mathbf{Y}_0;t)=p_F\cos\theta_0 \times \tilde{P}_{\rm sys}(\mathbf{Y};\mathbf{Y}_0;t)$, and $\tilde{P}_{\rm sys}(\mathbf{Y},\mathbf{Y}_0;t)$ and $\tilde{P}_{\rm env}(\mathbf{Q},\mathbf{Q}_0;t)$ are the classical probability densities. For the system, we need to take into account the fact that particles are injected, which is why the classical probability density must be multiplied with the initial system momentum $p_F\cos\theta_0$ along the injection lead.[64] The phase points $\mathbf{Y}_0=(y_0,\theta_0)$ and $\mathbf{Y}=(y,\theta)$ are at the boundary between the system and the leads. In contrast, $\mathbf{Q}_0=(\mathbf{q}_0,\mathbf{p}_0)$ and $\mathbf{Q}=(\mathbf{q},\mathbf{p})$ are inside the closed environment cavity. The momenta are integrated over the entire environment phase space, while $\tilde{P}_{\rm env}(\mathbf{Q},\mathbf{Q}_0;t)$ will always contain a δ function which restricts the final energy to equal the initial one (i.e., $|\mathbf{p}|=|\mathbf{p}_0|$ if all N environment particles have the same mass).

The average of $P_{\rm sys}$ over an ensemble of systems or over energy gives a smooth function. For a chaotic system, we write

$$\langle \tilde{P}_{\rm sys}(\mathbf{Y};\mathbf{Y}_0;t)\rangle = \frac{\cos\theta}{2(W_L+W_R)\tau_D} e^{-t/\tau_D}. \quad (16a)$$

Likewise, the average of $\tilde{P}_{\rm env}$ gives

$$\langle \tilde{P}_{\rm env}(\mathbf{Q};\mathbf{Q}_0;t')\rangle = \frac{\delta(|\mathbf{p}|-|\mathbf{p}_0|)}{\Xi_{\rm env}^{|\mathbf{p}_0|}}, \quad (16b)$$

where $\Xi_{\rm env}^{|\mathbf{p}_0|}$ is the size of the hypersurface in the environment's phase space defined by $|\mathbf{p}|=|\mathbf{p}_0|$ [for $d=2$, $\Xi_{\rm env}^{|\mathbf{p}_0|}=(2\pi p_F^{\rm env}\Omega_{\rm env})^N$ where $\Omega_{\rm env}$ is the area of the environment]. Inserting Eqs. (15a), (15b), (16a), and (16b) into Eq. (14), we can perform all integrals using $\int_{\rm env} d\mathbf{Q}_0 \equiv \int_{\rm env} d\mathbf{q}_0 d\mathbf{p}_0 = \Xi_{\rm env}$ and $\int_{\rm env} d\mathbf{Q}\,\delta(|\mathbf{p}|-|\mathbf{p}_0|) = \Xi_{\rm env}^{|\mathbf{p}_0|}$. Then, since $N_{L,R}=k_F W_{L,R}/\pi$, we recover the classical Drude conductance,

$$g^D = \frac{N_L N_R}{N_L+N_R}. \quad (17)$$

C. Overview of the effect of environment on weak localization

The leading-order weak-localization corrections to the conductance were identified in Refs. 14, 55, and 70 as those arising from trajectories that are paired almost everywhere except in the vicinity of an encounter. An example of such a trajectory is shown in Fig. 2. At the encounter, one of the trajectories (γ') intersects itself, while the other one (γ) avoids the crossing. Thus, they travel along the loop they form in opposite directions. For chaotic ballistic systems in the semiclassical limit, only pairs of trajectories with small crossing angle ϵ contribute significantly to weak localization. In this case, trajectories remain correlated for some time on both sides of the encounter, the correlated region indicated in pink in Fig. 2. In other words, the smallness of ϵ requires two minimal times, $T_L(\epsilon)$ to form a loop and $T_W(\epsilon)$ in order for the legs to separate before escaping into different leads. In the case of a hyperbolic dynamics, one estimates[71]

$$T_L(\epsilon) \simeq \lambda^{-1} \ln[\epsilon^{-2}], \quad (18a)$$

$$T_W(\epsilon) \simeq \lambda^{-1} \ln[\epsilon^{-2}(W/L)^2]. \quad (18b)$$

As long as the system-environment coupling does not generate energy and/or momentum relaxation, the presence of an environment does not significantly change this picture. However, it does lead to dephasing via the accumulation of uncorrelated action phases, mostly along the loop, when γ and γ' are more than a distance ξ apart. This is illustrated in Fig. 2 for the case when ξ is less than W. We define a new time scale T_ξ as twice the time between the encounter and the start of the dephasing,

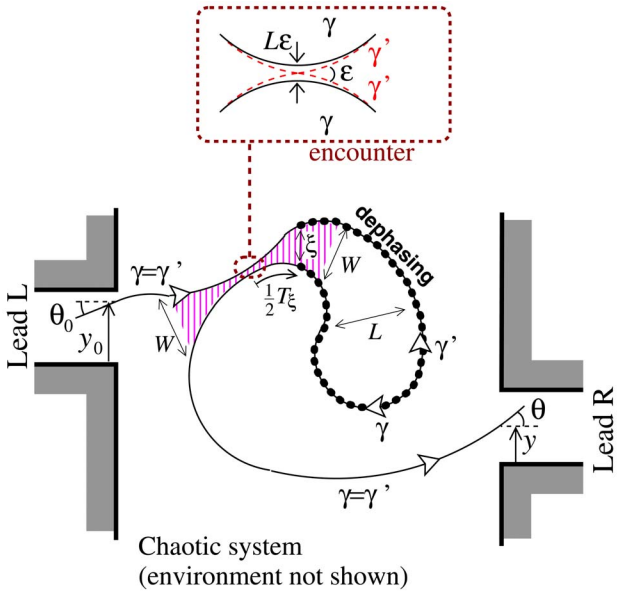

FIG. 2. (Color online) A semiclassical contribution to weak localization for the system-environment model. The paths are paired everywhere except at the encounter, where one path crosses itself at angle ϵ, while the other one does not (going the opposite way around the loop). Here, we show $\xi > \epsilon L$, so the dephasing (dotted path segment) starts in the loop ($T_\xi > 0$).

$$T_\xi(\epsilon) \approx \lambda^{-1} \ln[\epsilon^{-2}(\xi/L)^2]. \tag{19}$$

Dephasing occurs mostly in the loop part. However, if $\xi < \epsilon L$ and $T_\xi < 0$, dephasing starts before the paths reach the encounter. We discuss this point in more detail below in Sec. II G.

D. Calculating the effect of the environment on weak localization

In the absence of dephasing, each weak-localization contribution accumulates a phase difference $\delta\Phi_{\rm sys} = E_F \epsilon^2/(\lambda\hbar)$.[55,70] In the presence of an environment, an additional action phase difference $\delta\Phi_{\mathcal{U}}$ is accumulated. Incorporating this additional phase into the calculation of weak localization does not require significant departure from the theory at $\mathcal{U}=0$. We extend the theory of Ref. 45 to account for this additional phase.

We follow the same route as for the Drude conductance, but now consider the pairs of paths described in Sec. II C above and shown in Fig. 2, while the environment is still treated within the diagonal approximation, $\Gamma' = \Gamma$. The sum rule of Eq. (15b) still applies. Though the sum over system paths is restricted to paths with an encounter, we can still write this sum in the form given in Eq. (15a), provided that the probability $P_{\rm sys}(\mathbf{Y}, \mathbf{Y}_0; t)$ is restricted to paths which cross themselves. To ensure this, we write

$$P_{\rm sys}(\mathbf{Y}, \mathbf{Y}_0; t) = p_F \cos\theta_0 \int_C d\mathbf{R}_2 d\mathbf{R}_1 \tilde{P}_{\rm sys}(\mathbf{Y}, \mathbf{R}_2; t - t_2) \times \tilde{P}_{\rm sys}(\mathbf{R}_2, \mathbf{R}_1; t_2 - t_1) \tilde{P}_{\rm sys}(\mathbf{R}_1, \mathbf{Y}_0; t_1). \tag{20}$$

Here, we use $\mathbf{R} = (\mathbf{r}, \phi)$, $\phi \in [-\pi, \pi]$, for phase-space points inside the cavity, while $\mathbf{Y}$ lies on the lead as before. We then restrict the probabilities inside the integral to trajectories which cross themselves at phase-space positions $\mathbf{R}_{1,2}$ with the first (second) visit to the crossing occurring at time t_1 (t_2). We can write $d\mathbf{R}_2 = v_F^2 \sin\epsilon dt_1 dt_2 d\epsilon$ and set $\mathbf{R}_2 = (\mathbf{r}_1, \phi_1 \pm \epsilon)$. Then, the weak-localization correction to the dimensionless conductance in the presence of an environment is given by

$$g^{\rm wl} = (\pi\hbar)^{-1} \int_L d\mathbf{Y}_0 \int d\epsilon \, {\rm Re}[e^{i\delta\Phi_{\rm sys}}] \langle F(\mathbf{Y}_0, \epsilon)\rangle, \tag{21a}$$

with

$$F(\mathbf{Y}_0, \epsilon) = 2v_F^2 \sin\epsilon \int_{T_L+T_W}^{\infty} dt \int_{T_L+T_W/2}^{t-T_W/2} dt_2 \int_{T_W/2}^{t_2-T_L} dt_1 \times p_F \cos\theta_0 \int_R d\mathbf{Y} \int_C d\mathbf{R}_1 \tilde{P}_{\rm sys}(\mathbf{Y}, \mathbf{R}_2; t - t_2) \times \tilde{P}_{\rm sys}(\mathbf{R}_2, \mathbf{R}_1; t_2 - t_1) \tilde{P}_{\rm sys}(\mathbf{R}_1, \mathbf{Y}_0; t_1) \times \int \frac{d\mathbf{Q} d\mathbf{Q}_0}{\Xi_{\rm env}} \tilde{P}_{\rm env}(\mathbf{Q}, \mathbf{Q}_0; t) \exp[i\delta\Phi_{\mathcal{U}}]. \tag{21b}$$

Comparison with Eq. (34) of Ref. 45 shows that the effect of the environment is entirely contained in the last line of Eq. (21b). At the level of the diagonal approximation for the environment, $\Gamma' = \Gamma$, one has

$$\delta\Phi_{\mathcal{U}} = \frac{1}{\hbar} \int_0^t d\tau \{\mathcal{U}[\mathbf{r}_\gamma(\tau), \mathbf{q}_\Gamma(\tau)] - \mathcal{U}[\mathbf{r}_{\gamma'}(\tau), \mathbf{q}_\Gamma(\tau)]\}, \tag{21c}$$

where $\mathbf{r}_\gamma(\tau)$ and $\mathbf{q}_\Gamma(\tau)$ parametrize the trajectories of the system and of the environment, respectively. We note that in the absence of coupling, $\delta\Phi_{\mathcal{U}} = 0$, the integral over the environment is 1, and we recover the weak-localization correction of an isolated system [cf. Eq. (35) of Ref. 45].

To evaluate Eqs. (21a)–(21c), we need the average effect of the environment on the system, after one has traced out the environment. For a single measurement, this average is an integral over all classical paths followed by the environment, starting from its initial state at the beginning of the measurement. We therefore also average over an ensemble of initial environment states or an ensemble of environment Hamiltonians which corresponds to performing many measurements. For compactness, we define $\langle\cdots\rangle_{\rm env}$ as this integral over environment paths and the ensemble averaging over the environment,

$$\langle \cdots \rangle_{\mathrm{env}} = \int \frac{d\mathbf{Q}d\mathbf{Q}_0}{\Xi_{\mathrm{env}}} \langle \tilde{P}_{\mathrm{env}}(\mathbf{Q};\mathbf{Q}_0;t)[\cdots]_{\mathbf{Q}_0} \rangle. \tag{22}$$

Without loss of generality, we assume that for all $\mathbf{r}$, the interaction $\mathcal{U}(\mathbf{r},\mathbf{q})$ is zero upon averaging over all $\mathbf{q}$. We can ensure that an arbitrary interaction fulfills this condition by moving any constant term in $\mathcal{U}$ into the system Hamiltonian (these terms do not lead to dephasing). Since the environment is ergodic, we have

$$\langle \mathcal{U}[\mathbf{r}_\gamma(t),\mathbf{q}_\Gamma(t)] \rangle_{\mathrm{env}} = 0. \tag{23}$$

Now, we use the chaotic nature of the environment to give the properties of the correlation function $\langle \mathcal{U}[\mathbf{r}_\gamma(t),\mathbf{q}_\Gamma(t)]\mathcal{U}[\mathbf{r}_{\gamma'}(t'),\mathbf{q}_\Gamma(t')] \rangle_{\mathrm{env}}$.

(i) Correlation functions typically decay exponentially fast with time in chaotic systems, with a typical decay time related to the Lyapunov exponent.[72] The precise functional form $J(\lambda_{\mathrm{env}}|t'-t|)$ of the temporal decay of the coupling correlator depends on details of H_{env} and $\mathcal{U}$; however, for all practical purposes, it is sufficient to know that it decays fast, and we approximate it by a δ function, $J(\lambda_{\mathrm{env}}|t'-t|) \simeq \lambda_{\mathrm{env}}^{-1}\delta(t)$.

(ii) We argue that the spatial correlations of $\mathcal{U}$ for two different system paths at the same t also decay because the averaging over many paths and many initial environment states act like an average over $\mathbf{q}$. We define $K(|\mathbf{r}'-\mathbf{r}|/\xi)$ as the functional form of this decay of spatial correlations, with $K(0)=1$. The precise form of $K(x)$ depends on details of H_{sys}, H_{env}, and $\mathcal{U}$. In particular, the typical length ξ of this decay is of order the scale on which $\mathcal{U}(\mathbf{r},\mathbf{q})$ changes between its maximum and minimum values.

Given these arguments, we have

$$\begin{aligned}\langle \mathcal{U}[\mathbf{r}_\gamma(t),\mathbf{q}_\Gamma(t)]\mathcal{U}[\mathbf{r}_{\gamma'}(t'),\mathbf{q}_\Gamma(t')] \rangle_{\mathrm{env}} \\ = \frac{\langle \mathcal{U}^2 \rangle}{\lambda_{\mathrm{env}}} K(|\mathbf{r}_{\gamma'}(t)-\mathbf{r}_\gamma(t)|/\xi)\delta(t-t').\end{aligned} \tag{24}$$

Then,

$$\begin{aligned}\langle \delta\Phi_{\mathcal{U}}^2 \rangle_{\mathrm{env}} &= \frac{1}{\hbar^2}\int_0^t d\tau_2 d\tau_1 \\ &\quad \big\langle \{\mathcal{U}[\mathbf{r}_\gamma(\tau_2),\mathbf{q}_\Gamma(\tau_2)] - \mathcal{U}[\mathbf{r}_{\gamma'}(\tau_2),\mathbf{q}_\Gamma(\tau_2)]\} \\ &\quad \times \{\mathcal{U}[\mathbf{r}_\gamma(\tau_1),\mathbf{q}_\Gamma(\tau_1)] - \mathcal{U}[\mathbf{r}_{\gamma'}(\tau_1),\mathbf{q}_\Gamma(\tau_1)]\} \big\rangle_{\mathrm{env}} \\ &= 2\frac{\langle \mathcal{U}^2 \rangle}{\lambda_{\mathrm{env}}}\int_0^t d\tau [1 - K(|\mathbf{r}_{\gamma'}(\tau)-\mathbf{r}_\gamma(\tau)|/\xi)].\end{aligned} \tag{25}$$

We further make the following step-function approximation for K:

$$K(x) = \Theta(1-x), \tag{26}$$

where the Euler Θ function is 1 (zero) for positive (negative) arguments. In principle, this is unjustifiable for $x \sim 1$; however, since the paths diverge exponentially from each other, the time during which $x \sim 1$ is of order λ^{-1}, while dephasing happens on a time scale τ_ϕ which is typically of order the dwell time, τ_D. Thus the step-function approximation of $K(x)$ will have corrections of order $(\lambda\tau_D)^{-1} \ll 1$, which we therefore neglect. Once we have made the approximation in Eq. (26), we see that nonzero contributions to $\langle \delta\Phi_{\mathcal{U}}^2 \rangle$ come from regions where the distance between γ and γ' is larger than ξ.

We are now ready to calculate dephasing for those system paths shown in Fig. 2. As defined above, t_1 and t_2 are the two times at which the path γ' crosses itself. Dephasing acts on the loop formed by γ' and, as just argued, it acts once the distance between γ and γ' is greater than ξ, i.e., in the time window from $(t_1+T_\xi/2)$ to $(t_2-T_\xi/2)$, where $T_\xi(\epsilon)$ is given in Eq. (19). We average Eq. (21b) over the environment and use the central limit theorem to evaluate the action phase due to the coupling between system and environment,

$$\langle \exp[i\delta\Phi_{\mathcal{U}}] \rangle_{\mathrm{env}} = \exp\left[-\tfrac{1}{2}\langle \delta\Phi_{\mathcal{U}}^2 \rangle_{\mathrm{env}}\right] = \exp[-(t_2-t_1-T_\xi)/\tau_\phi], \tag{27}$$

where the dephasing rate is

$$\tau_\phi^{-1} \sim \hbar^{-2}\lambda_{\mathrm{env}}^{-1}\langle \mathcal{U}^2 \rangle. \tag{28}$$

Given that $\langle \cdots \rangle_{\mathrm{env}}$ is defined in Eq. (22), we can substitute Eq. (27) directly into Eqs. (21a)–(21c). We thereby reduce the problem to an integral over system paths, which is almost identical to the equivalent integral for $\mathcal{U}=0$. Assuming phase-space ergodicity for the system, we get the probabilities

$$\langle \tilde{P}_{\mathrm{sys}}(\mathbf{R}_1,\mathbf{Y}_0;t_1) \rangle = \frac{e^{-t_1/\tau_D}}{2\pi\Omega_{\mathrm{sys}}}, \tag{29a}$$

$$\langle \tilde{P}_{\mathrm{sys}}(\mathbf{R}_2,\mathbf{R}_1;t_2-t_1) \rangle = \frac{e^{-(t_2-t_1-T_W/2)/\tau_D}}{2\pi\Omega_{\mathrm{sys}}}, \tag{29b}$$

$$\langle \tilde{P}_{\mathrm{sys}}(\mathbf{Y},\mathbf{R}_2;t-t_2) \rangle = \frac{\cos\theta e^{-(t-t_2-T_W/2)/\tau_D}}{2(W_L+W_R)\tau_D}, \tag{29c}$$

with Ω_{sys} being the real space volume occupied by the system (the area of the cavity). At this point, the integral is the same as without dephasing, except that during the time $(t_2-t_1-T_\xi)$, the inverse dwell time is replaced by $(\tau_D^{-1}+\tau_\phi^{-1})$. Thus, when evaluating the (t_2-t_1) integral, we get the extra prefactor $\exp[-T_L(\epsilon)/\tau_\phi]/(1+\tau_D/\tau_\phi)$ compared with the equivalent integral result without dephasing. Thus, we have

$$\langle F(\mathbf{Y}_0,\epsilon) \rangle \propto \sin\epsilon \frac{e^{-T_L(\epsilon)/\tau_D - [T_L(\epsilon)-T_\xi(\epsilon)]/\tau_\phi}}{1+\tau_D/\tau_\phi}. \tag{30}$$

Since $[T_L(\epsilon)-T_\xi(\epsilon)]=\tau_\xi$ with τ_ξ defined in Eq. (4), the ϵ dependence of the τ_ϕ^{-1} term drops out. This means that $\langle F(\mathbf{Y}_0,\epsilon) \rangle$ simply differs from its value without dephasing by a constant factor, $e^{-\tau_\xi/\tau_\phi}/(1+\tau_D/\tau_\phi)$. Thus, the integral over ϵ in Eq. (21a) is identical to the one in the absence of the environment and takes the form[45] $\mathrm{Re}\int_0^\infty d\epsilon \epsilon^{1+2/(\lambda\tau_D)} \exp[iE_F\epsilon^2/(\lambda\hbar)]$, where we have assumed $\epsilon \ll 1$. The substitution $z=E_F\epsilon^2/(\lambda\hbar)$ immediately yields a dimensionless integral and an exponential term, $e^{-\tau_E^{\mathrm{cl}}/\tau_D}$ (neglecting as usual $\mathcal{O}[1]$ terms in the logarithm in τ_E^{cl}). From this analysis, we find that the weak-localization correction is given by

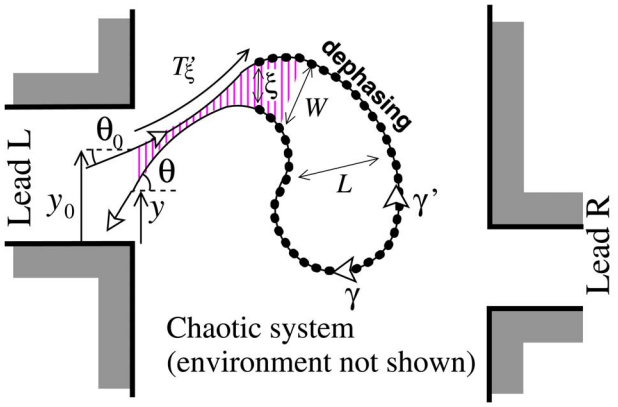

FIG. 3. (Color online) A semiclassical contribution to coherent backscattering for the system-environment model. It involves paths which return to close, but antiparallel to themselves at lead L. The two solid paths are paired (within W of each other) in the cross-hatched region. Here, we show $\xi > \epsilon L$, so the dephasing (dotted path segment) starts in the loop ($T_\xi > 0$). In the basis parallel and perpendicular to γ at injection, the initial position and momentum of path γ at exit are $r_{0\perp}=(y_0-y)\cos\theta_0$, $r_{0\parallel}=(y_0-y)\sin\theta_0$, and $p_{0\perp}=p_F(\theta-\theta_0)$.

$$g^{\rm wl} = \frac{g_0^{\rm wl}}{1+\tau_D/\tau_\phi}\exp[-\tau_\xi/\tau_\phi], \tag{31}$$

where $g_0^{\rm wl}$ is the weak-localization correction at finite $\tau_E^{\rm cl}$ in the absence of dephasing,

$$g_0^{\rm wl} = -\frac{N_L N_R}{(N_L+N_R)^2}\exp[-\tau_E^{\rm cl}/\tau_D]. \tag{32}$$

We see that the dephasing of weak localization is not exponential with the Ehrenfest time; instead, it is exponential with the λ_F-independent scale τ_ξ given in Eq. (4). In all cases where ξ is a classical scale (i.e., of similar magnitude to W, L rather than λ_F), we see that τ_ξ is much less than the Ehrenfest time, $\tau_\xi \ll \tau_\phi$. In such cases, the exponential term in Eq. (31) is much less noticeable than the universal power-law suppression of weak localization.

E. Weak localization for reflection and coherent backscattering

We show explicitly that our semiclassical method is probability conserving and thus current conserving, also in the presence of dephasing. We do this by calculating the leading-order quantum corrections to reflection, showing that they enhance reflection by exactly the same amount that transmission is reduced. There are two leading-order off-diagonal corrections to reflection. The first one reduces the probability of reflection to arbitrary momenta (weak localization for reflection), while the second one enhances the probability of reflection to the time reversed of the injection path (coherent backscattering). The distinction between these two contributions is related to the correlation between the path segments when they hit the leads. For coherent-backscattering contributions, these segments are correlated (see Fig. 3), but for weak localization contributions, they are not.

The derivation of the weak localization for reflection $r^{\rm wl}$ is straightforward and proceeds in the same way as the derivation for $g^{\rm wl}$ given above, replacing the factor $N_R/(N_R+N_L)$ by $N_L/(N_R+N_L)$. We thus get

$$r^{\rm wl} = \frac{r_0^{\rm wl}}{1+\tau_D/\tau_\phi}\exp[-\tau_\xi/\tau_\phi], \tag{33}$$

where $r_0^{\rm wl}=-\exp[-\tau_E^{\rm cl}/\tau_D]N_L^2/(N_L+N_R)^2$ is the finite-$\tau_E^{\rm cl}$ correction in the absence of dephasing.

We next calculate the contributions to coherent backscattering, extending the treatment of Ref. 45 to account for the presence of dephasing. As before, the environment is treated in the diagonal approximation. The coherent-backscattering contributions correspond to trajectories where legs escape together within $T_W/2$ of the encounter. Such a contribution is shown in Fig. 3. The correlation between the system paths at injection and exit induces an action difference $\delta\Phi_{\rm sys}=\delta S_{cbs}$ not given by the Richter-Sieber expression. It is convenient to write this action difference in terms of relative coordinates at the lead (rather than at the encounter). The system action difference is then $\delta S_{cbs}=-(p_{0\perp}+m\lambda r_{0\perp})r_{0\perp}$, where the perpendicular difference in position and momentum are $r_{0\perp}=(y_0-y)\cos\theta_0$ and $p_{0\perp}=p_F(\theta-\theta_0)$. As with weak localization, we can identify three time scales, T'_L, T'_W, T'_ξ, associated with the time for paths to spread to each of three length scales, L, W, ξ. However, unlike for weak localization, we define these time scales as a time measured from the lead rather than from the encounter. Thus, we have

$$T'_\ell(r_{0\perp},p_{0\perp}) \simeq \lambda^{-1}\ln[(m\lambda\ell)^2/|p_{0\perp}+m\lambda r_{0\perp}|^2], \tag{34}$$

with $\ell=\{L,W,\xi\}$. Writing the integral over $\mathbf{Y}_0$ as an integral over $(r_{0\perp},p_{0\perp})$ and using $p_F\sin\theta_0 d\mathbf{Y}_0 = dp_{0\perp}dr_{0\perp}$, the coherent-backscattering contribution is

$$r^{\rm cbs} = \int_L \frac{dp_{0\perp}dr_{0\perp}}{p_F\sin\theta_0}{\rm Re}[e^{i\delta S_{\rm cbs}}]\langle F^{\rm cbs}(\mathbf{Y}_0)\rangle. \tag{35}$$

After integrating out the environment in the same manner as for weak localization, we get

$$F^{\rm cbs}(\mathbf{Y}_0) = \int_L d\mathbf{Y}\int_{T'_L}^{\infty} dt\langle P_{\rm sys}(\mathbf{Y},\mathbf{Y}_0,t)\rangle\exp[-(t-T'_\xi)/\tau_\phi]$$
$$= \frac{N_L p_F\sin\theta_0}{\pi(N_L+N_R)}\frac{\exp[-(T'_L-T'_W/2)/\tau_D-(T'_L-T'_\xi)/\tau_\phi]}{1+\tau_D/\tau_\phi}. \tag{36}$$

Now, we can proceed as for $\mathcal{U}=0$, pushing the momentum integral's limits to infinity and evaluating the $r_{0\perp}$ integral over the range W, with the help of a Euler Γ function. We finally obtain

$$r^{\rm cbs} = \frac{r_0^{\rm cbs}}{1+\tau_D/\tau_\phi}\exp[-\tau_\xi/\tau_\phi], \tag{37}$$

in terms of $r_0^{\rm cbs}=\exp[-\tau_E^{\rm cl}/\tau_D]\ N_L/(N_L+N_R)$, the finite-$\tau_E^{\rm cl}$ coherent-backscattering contribution in the absence of

dephasing. Hence, $r^{\mathrm{cbs}}+r^{\mathrm{wl}}=-g^{\mathrm{wl}}$ for all values of τ_ξ and τ_ϕ, and our approach is probability and thus current conserving.

F. Weak-localization corrections in the environment

So far, we have only considered cases where we make a diagonal approximation for the environment. On the face of it, this seems a little unreasonable. For instance, if the system and environment are of similar sizes, then one would expect that diagonal contributions for the system and weak localization for the environment would be as important as the contributions calculated above.

Since the environment is a closed cavity, one would naively think that the weak-localization contribution for the environment should be calculated in a similar manner to the form factor in Refs. 70 and 73. In the absence of coupling, the environment part of Eq. (12) would then be

$$\int \frac{d\mathbf{q}d\mathbf{q}_0}{\Xi_{\mathrm{env}}} \sum_{\Gamma,\Gamma'} A_\Gamma A_{\Gamma'} e^{i\Phi_{\mathrm{env}}} = 1 + \mu \frac{\Delta_{\mathrm{env}} t}{\hbar}, \tag{38}$$

where μ is a number of order 1 and Δ_{env} is the environment level spacing (for a two-dimensional environment containing a single particle, $\Delta_{\mathrm{env}} \sim \hbar^2/mL_{\mathrm{env}}^2$). The first term above comes from the diagonal approximation used throughout this paper, while the second term is a weak-localization correction. This correction becomes of order the system's weak-localization correction on the time scale $t \sim \tau_D$, so there is *a priori* no reason to neglect it.

The environment part of our calculation differs, however, from the form factor in that it corresponds to the time evolution of the environment during the time it takes for a particle to be transported across the system. Therefore, the sum in Eq. (38) is not restricted to periodic orbits, and the unitarity of the environment's time evolution imposes that $\mu=0$. Furthermore, unitarity must be preserved even in the presence of a finite $\mathcal{U}$, as long as there is no exchange of particles between system and environment. We thus conclude that we do not need to consider the weak-localization-type corrections to the environment evolution because they cancel.

G. Regime of validity of the semiclassical calculation

Throughout this paper, we assumed that the system-environment coupling is weak enough not to modify the classical paths in the system. Formally, this assumption can be rigorously justified by invoking theorems on structural stability.[74] However, care should be taken in extrapolating our results to the limit $\xi \to 0$ since the force on the particle is the gradient of the interaction potential, $\sim U/\xi$. We therefore estimate the minimum ξ for which we can legitimately assume that classical system paths are left unchanged by the system-environment coupling. This will give the bound on the regime of validity of our approach.

To see significant dephasing, we need $\tau_\phi \sim \tau_D$, so we cannot take the interaction strength to zero; instead, we require that $\langle U^2 \rangle \sim \lambda_{\mathrm{env}} \hbar^2/\tau_D$, see Eq. (28). This induces a typical force $\sim \langle U^2 \rangle^{1/2}/\xi \sim (\hbar/\xi)(\lambda_{\mathrm{env}}/\tau_D)^{1/2}$ on the particle. To see if this noisy force significantly modifies the paths in the vicinity of the encounter, we compare it with the relative force

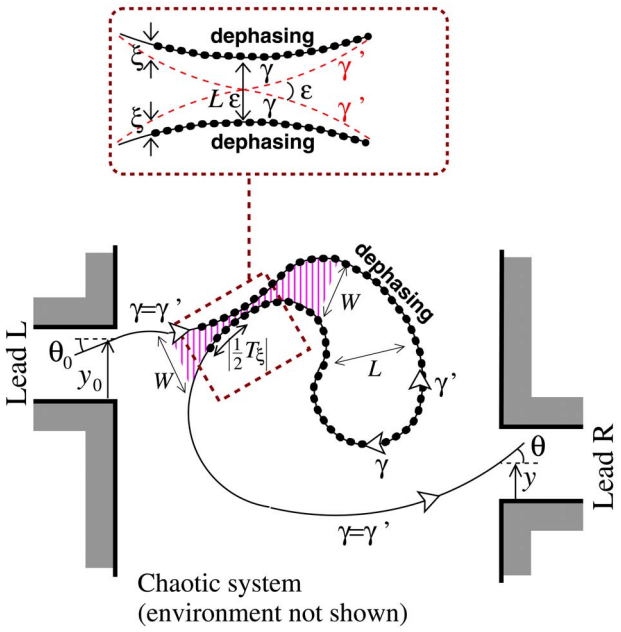

FIG. 4. (Color online) Dephasing of weak localization when $\xi \ll L\epsilon \sim (L\lambda_F)^{1/2}$, and hence $T_\xi(\epsilon)$ is negative, see Eq. (19). The dephasing starts and ends in the "legs" rather than the loop. In the language of disordered systems, this means that the dephasing affects the diffusons as well as the cooperon.

of the chaotic system Hamiltonian on the particle at the encounter. Since the perpendicular extension of the encounter is $\delta r_\perp \sim (L\lambda_F)^{1/2}$ and the duration of the encounter is of order the Lyapunov time $\sim \lambda^{-1}$, the system force goes like $m\lambda^2 \delta r_\perp \sim m\lambda^2 (L\lambda_F)^{1/2}$. Estimating $\lambda^{-1} \sim v_F/L$ as is typical of chaotic billiards, the ratio of the noisy force to the system force becomes $[\lambda_{\mathrm{env}} L\lambda_F/(\xi^2 \lambda^2 \tau_D)]^{-1/2}$. Thus, one can ignore the modifications of the classical paths due to the coupling to the environment, as long as

$$\xi \gg (\lambda_F L)^{1/2} \left[\frac{\lambda_{\mathrm{env}}/\lambda}{\lambda \tau_D} \right]^{1/2}. \tag{39}$$

We see that ξ can easily be less than the typical encounter size $\delta r_\perp \sim (L\lambda_F)^{1/2}$ (remember that $\lambda \tau_D \gg 1$ is always assumed). Thus, our method is not only applicable for ξ up to the system size, where dephasing happens only in the loop. It is also applicable for ξ smaller than the encounter size, in which case the time $T_\xi(\epsilon)$ is negative, and dephasing occurs in part of the legs as well as the whole of the loop, see Fig. 4.

Finally, we caution the reader that the whole semiclassical method used in this paper relies on the lead width being greater than the encounter size, this requires that $\lambda \tau_D \ll (L/\lambda_F)^{1/2}$; thus, we *cannot* access the regime $\xi \sim \lambda_F$, which is dominated by stochastic diffraction at the leads.

H. Shot noise in the presence of an environment

When the temperature of the electrons in the leads coupled to a chaotic system is taken to zero, there is no

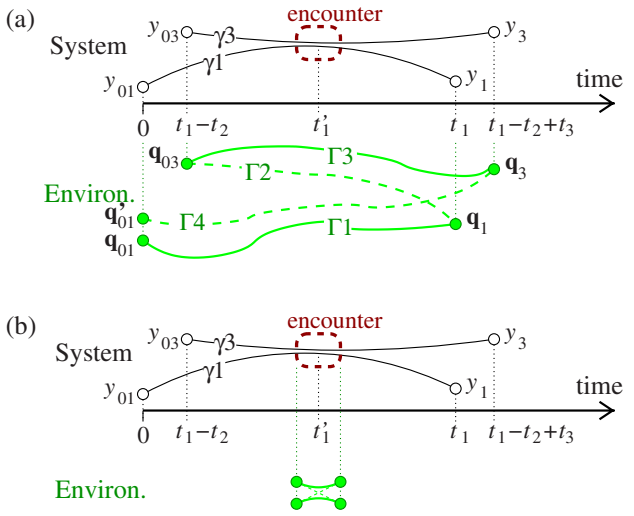

FIG. 5. (Color online) Sketch of typical trajectories which contribute to shot noise in the presence of an environment. In both (a) and (b), the system (environment) paths are sketched above (below) the time axis. In (a), we show a contribution which will survive system averaging because the system paths are paired almost everywhere with an encounter at time t_1'. There is no constraint on the environment paths, as yet. For simplicity, we show only system paths $\gamma 1$ and $\gamma 3$, with paths $\gamma 2$ and $\gamma 4$ being the same as $\gamma 1$ and $\gamma 3$ except that they cross at the encounter. Depending on the choice of t_1' with respect to the other time scales, t_1, t_2, t_3, this pair of system paths could represent any of the contributions in Fig. 1 of Ref. 50. In (b), additional constraints are imposed on the Γ_i's, after one has integrated over all initial and final positions of the environment. This integration removes all contributions from *environment* propagation when the *system* paths are paired.

thermal noise in the current through the device. However, there is still the intrinsically quantum noise which originates from the wavelike nature of the electrons. This zero-temperature noise is known as shot noise.[83] In the absence of dephasing, shot noise has been well studied using RMT,[35] quasiclassical field theory,[47] and semiclassical methods.[49,75,50]

It is generally argued that the shot noise is unaffected by the presence of an environment which causes dephasing but not heating of the electrons—the regime of *phase breaking* of Ref. 57. This belief is founded on the fact that (i) the dephasing-lead model gives a dephasing-independent shot noise and (ii) kinetic equations—in which interference effects are ignored—give the same shot noise as full quantum calculations. Here, we show explicitly that, under the assumption that the system-environment coupling does not heat up the current-carrying electrons, indeed, the coupling to the environment does not affect shot noise.

We start with the formula for the zero-frequency shot noise power through a system coupled to an environment. This formula is derived in the Appendix and is given as $S_{RR}(0)$ in Eq. (A17). We use Eq. (11) to write each matrix element as sums over classical paths. This gives us a sum over eight paths—four system paths and four environment paths—as sketched in Fig. 5. The system paths are as follows:

(1) $\gamma 1$ from y_{01} on lead L to y_1 on lead R;
(2) $\gamma 2$ from y_{03} on lead R to y_1 on lead R;
(3) $\gamma 3$ from y_{03} on lead R to y_3 on lead R;
(4) $\gamma 4$ from y_{01} on lead L to y_3 on lead R.

The sums over lead modes and the trace over the environment density matrix are performed in the same manner as for the conductance [see Eq. (12)], which results in

$$S = \frac{e^3 V}{(2\pi\hbar)^3}\int_L dy_{01}\int_R dy_{03}dy_1 dy_3 \sum_{\gamma 1,\ldots,\gamma 4} A_{\rm sys} e^{i\Phi_{\rm sys}} \times \int d\mathbf{q}_{01}d\mathbf{q}_{03}d\mathbf{q}_1 d\mathbf{q}_3 \sum_{\Gamma 1,\ldots,\Gamma 4} A_{\rm env} e^{i(\Phi_{\rm env}+\Phi_{\mathcal{U}})}. \quad (40)$$

Here, $A_{\rm sys}=A_{\gamma 1}A_{\gamma 2}A_{\gamma 3}A_{\gamma 4}$, $\Phi_{\rm sys}=(S_{\gamma 1}-S_{\gamma 2}+S_{\gamma 3}-S_{\gamma 4})/\hbar$, and we absorbed all Maslov indices into the actions. Similarly, $A_{\rm env}=A_{\Gamma 1}A_{\Gamma 2}A_{\Gamma 3}A_{\Gamma 4}$, $\Phi_{\rm env}=(S_{\Gamma 1}-S_{\Gamma 2}+S_{\Gamma 3}-S_{\Gamma 4})/\hbar$, and $\Phi_{\mathcal{U}}=(\mathcal{S}_{\gamma 1,\Gamma 1}-\mathcal{S}_{\gamma 2,\Gamma 2}+\mathcal{S}_{\gamma 3,\Gamma 3}-\mathcal{S}_{\gamma 4,\Gamma 4})/\hbar$. As argued above, in the regime of pure dephasing, $\Phi_{\rm sys}$, $\Phi_{\rm env}$, and $\Phi_{\mathcal{U}}$ are uncorrelated. We thus first pair up the system paths to minimize $\Phi_{\rm sys}$; this pairing is the same as it would be in the absence of the environment (compare Fig. 5 to Fig. 1 of Ref. 50). We see from the construction of Eq. (A17) that all paths reach the encounter at the same time,[76] t_1'.

Now, we make the crucial observation that, for any given set of system paths, we have $\gamma 1 \simeq \gamma 2$ for times greater than t_1'. Thus, for times greater than t_1', we can write the sum over $\Gamma 1$, $\Gamma 2$ in the second line of Eq. (40) as

$$\int d\mathbf{q}_1 \sum_{\Gamma 1,\Gamma 2} A_{\Gamma 1}A_{\Gamma 2} e^{i(S_{\Gamma 1}-S_{\Gamma 2}+\mathcal{S}_{\gamma 1,\Gamma 1}-\mathcal{S}_{\gamma 2,\Gamma 2})/\hbar} \simeq \int d\mathbf{q}_1 \sum_{\Gamma 1,\Gamma 2} A_{\Gamma 1}A_{\Gamma 2} e^{i(S_{\Gamma 1}-S_{\Gamma 2}+\mathcal{S}_{\gamma 1,\Gamma 1}-\mathcal{S}_{\gamma 1,\Gamma 2})/\hbar} = \int d\mathbf{q}_1 [\mathcal{K}'_{\rm env}(\mathbf{q}_1,t_1;\mathbf{q}_1'',t_1')]^* \mathcal{K}'_{\rm env}(\mathbf{q}_1,t_1;\mathbf{q}_1',t_1'), \quad (41)$$

where we set $\gamma 2=\gamma 1$ to get the second line. We define $\mathcal{K}'_{\rm env}(\mathbf{q}_1,t_1;\mathbf{q}_1',t_1')$ as the propagator for the environment evolving under an effective time-dependent potential, $V'(q,t)$, which is the sum of $\mathcal{U}[r_{\gamma 1}(t),q]$ and the potential term in $H_{\rm env}$. Since both propagators in Eq. (41) evolve under the same potential (because $\gamma 1=\gamma 2$), we can use the basic property of propagators[77] that

$$\int d\mathbf{q}_1 [\mathcal{K}'_{\rm env}(\mathbf{q}_1,t_1;\mathbf{q}',t_1')]^* \mathcal{K}'_{\rm env}(\mathbf{q}_1,t_1;\mathbf{q}'',t_1') = \delta(\mathbf{q}''-\mathbf{q}') \quad (42)$$

to integrate out these propagators for times greater than t_1'. In their place, we have a constraint that paths $\Gamma 1$ and $\Gamma 2$ must be the same at time t_1'. This is sketched in Fig. 5; the paths $\Gamma 1$ and $\Gamma 2$ to the right of the encounter in Fig. 5(a) are replaced in Fig. 5(b) by the constraint that paths $\Gamma 1$ and $\Gamma 2$ meet at time t_1'. Note that we cannot use Eq. (42) to integrate out paths $\Gamma 1$ and $\Gamma 2$ for arbitrary times before t_1' because the system paths $\gamma 1$ and $\gamma 2$ are then different enough that the potential $V'(q,t)$ will be different for the two propagators in Eq. (41). However, we can use the same argument to inte-

grate out the pair Γ3-Γ4 after time t_1' and to integrate out the pairs Γ1-Γ4 and Γ2-Γ3 *before* the time t_1'. After all these pairs are replaced by δ functions, we get the situation shown in Fig. 5(b).

Focusing on ξ much greater than the encounter size, the above method can be used to integrate out the environment paths for all $t>t_1'$ and all $t<t_1'$. This leaves a single point (the environment state at $t=t_1'$) to integrate over. Doing this, we see that Eq. (40) reduces to

$$S = \frac{e^3 V}{(2\pi\hbar)^3} \int_L dy_{01} \int_R dy_{03} dy_1 dy_3 \sum_{\gamma 1,\ldots,\gamma 4} A_{\rm sys} e^{i\Phi_{\rm sys}}. \quad (43)$$

This is identical to the shot noise formula in the absence of an environment. Thus, we have completely removed the environment from the problem without affecting the shot noise of the system at all. To calculate the shot noise now, one simply needs to follow the derivation for a system without an environment in Ref. 50. The result is most conveniently written in terms of the Fano factor F, which is the ratio of the shot noise to the Poissonian noise $2e\langle I\rangle$, where $\langle I\rangle = 2e^2 g^D V/h$ is the average current. One gets

$$F \equiv S/2e\langle I\rangle = \frac{N_L N_R}{(N_L+N_R)^2} \exp[-\tau_E^{\rm op}/\tau_D]. \quad (44)$$

This is of course independent of the coupling to the environment.

As a final comment, we note that above, we kept only the leading $\mathcal{O}[N]$ term in the shot noise. There is a hierarchy of weak-localization-like corrections $\mathcal{O}[N^a]$, $a=0,-1,\ldots$, to this result,[75] which are suppressed by dephasing in much the same way as the weak-localization correction to conductance. Thus, for $\tau_E^{\rm op} \ll \tau_D$, we can expect the environment to cause a crossover from the result in Ref. 75 to the result in Eq. (44) with $\tau_E^{\rm op}=0$. Hence, in the classical limit of wide leads ($N_{L,R} \gg 1$), the environment's effect is negligible; however, for narrow leads ($N_{L,R} \sim 1$), the environment's effect may be significant.

III. CLASSICAL NOISE

We have shown that, to capture the effect of dephasing on weak localization, it is sufficient to treat the environment at the level of the diagonal approximation. We thus observe that, in the semiclassical limit of short wavelength, $\lambda_F/L_{\rm env} \to 0$, a quantum chaotic environment has the same dephasing effect on weak localization as the equivalent *classical* chaotic environment. Because correlations typically decay exponentially fast in classical hyperbolic systems, this makes the effect of this classical environment very similar to a classical-noise field with a suitably chosen spatial and temporal correlation function. In this section, we show that the conclusions that we draw for a quantum environment can also be drawn for a classical-noise field. One common experimental example of such a field is microwave radiation, applied to the chaotic dot either by accident or on purpose.[27] A second example is the common theoretical treatment of electron-electron interactions as a source of classical (Johnson-Nyquist) noise.[8,9]

We add a new term to the system Hamiltonian of the form $V_{\rm noise}(t)$. We assume that this term is weak enough that it does not affect the classical paths, but strong enough to modify the phase acquired along such paths. The phase difference for a pair of paths contributing to the conductance is $(\Phi_{\rm sys}+\Phi_{\rm noise})$, where $\Phi_{\rm sys}$ is given in Eq. (13a) and

$$\Phi_{\rm noise} = \int dt[V(\mathbf{r}_{\gamma'};t) - V(\mathbf{r}_{\gamma};t)]/\hbar. \quad (45)$$

We now assume that the noise is Gaussian distributed with

$$\langle V[\mathbf{r}_{\gamma'}(t);t]V[\mathbf{r}_{\gamma}(t');t']\rangle = \langle V^2\rangle K_{\rm noise}(|\mathbf{r}_2-\mathbf{r}_1|/\xi) \times J_{\rm noise}(\lambda_{\rm noise}|t_2-t_1|). \quad (46)$$

Here, $K_{\rm noise}(x)$ gives the form of the spatial decay of the correlation function (on a scale ξ) and $J_{\rm noise}(t)$ gives the form of the temporal decay of the correlation function (on a scale which we call $\lambda_{\rm noise}^{-1}$ to make the analogy with the notation in Sec. II C). We can now follow the derivation in Sec. II C by replacing $\mathcal{U}[\mathbf{r}_\gamma(t),\mathbf{q}_\Gamma(t)]$ with $V(\mathbf{r}_\gamma;t)$ throughout. We assume that the correlations in time are short enough to be treated as white-noise-like, $J_{\rm noise}(x) \propto \delta(x)$, and that the spatial correlations decay fast enough that we can justify the approximation in Eq. (26). This directly leads to the same result for weak localization as in Eq. (31), where now

$$\tau_\phi^{-1} \sim \hbar^{-2} \lambda_{\rm noise}^{-1} \langle V^2\rangle. \quad (47)$$

A. Noise due to electron-electron interactions in a two-dimensional ballistic system

Here, we consider the noise generated by electron-electron interactions in a ballistic chaotic system. In such a system, dephasing is caused by noise with momenta (δp vectors) larger than the inverse system size, L^{-1}. Thus, the dephasing processes are the same as those for ballistic motion in disordered systems (δp vectors greater than the inverse mean free path). Such processes were first studied in Ref. 13 for spinless electrons, while more recently Ref. 15 explored the full crossover from ballistic to diffusive motion for electrons with spin. The effect of a finite Ehrenfest time on such dephasing was considered in Ref. 24, which found that the dephasing rate in the vicinity of the encounter has a logarithmic dependence on the perpendicular distance between paths. This led them to observe that the electron-electron interaction in a two-dimensional ballistic system dephases weak localization exponentially with the Ehrenfest time. We repeat their derivation here and show that

$$g_{\rm e\text{-}e}^{\rm wl} = \frac{g_0^{\rm wl}}{1+\tau_D/\tau_\phi} \exp\left[-\left(\tau_E^{\rm cl} + \frac{1}{2}\tau_{L_T}\right) \Big/ \tau_\phi\right], \quad (48)$$

where τ_{L_T} is given by Eq. (31) with ξ equaling a thermal length scale $L_T = \hbar v_F/k_B T$. Reference 24 neglected the τ_{L_T} term in the exponent since it is often small.

In our qualitative derivation of this result, we treat the electron-electron interaction as classical noise rather than using the perturbative field theory approach in Refs. 13, 15, and 24. Our approach is similar in spirit to those for diffusive

systems.[8,9] The screened electron-electron interaction gives a correlation function of the form[13]

$$\langle V^2_{\delta p,\omega}\rangle \propto \frac{\delta(\omega - m^{-1}\mathbf{p}\cdot\delta\mathbf{p})}{|\delta\mathbf{p}|}J(\omega), \tag{49}$$

where we assume that $|\delta\mathbf{p}| \ll |\mathbf{p}|$, so the energy difference between a particle with momentum $(\mathbf{p}+\delta\mathbf{p})$ and $\mathbf{p}$ is $\mathbf{p}\cdot\delta\mathbf{p}/m$. The factor of $1/|\delta\mathbf{p}|$ comes from the imaginary part of the screened Coulomb interaction, is due to the polarization bubble, and corresponds to the fluctuations of the electron sea at momentum and frequency $(\delta p, \omega)$. The δ function ensures that energy and momentum are conserved in the interaction between the system and the environment. The function $J(\omega)$ gives the weight of environment modes excited at energy ω. At temperature T, it is typically of the form $J(\omega) \approx [\sinh(\omega/k_BT)]^{-1}$. It is convenient to write $\delta\mathbf{p}$ in terms of components parallel and perpendicular to the relevant classical path, i.e., parallel and perpendicular to $\mathbf{p}$. Then,

$$\langle V^2_{\delta p,\omega}\rangle \propto \frac{\delta(\omega - v_F\delta p_\parallel)}{[\delta p_\parallel^2 + \delta p_\perp^2]^{1/2}}J(\omega), \tag{50}$$

and we have

$$\langle V[\mathbf{r}_{\gamma'}(t');t']V[\mathbf{r}_\gamma(t);t]\rangle = \int d^d\delta\mathbf{p}\int d\omega e^{i[\delta\mathbf{p}\delta\mathbf{r}(t',t)+\omega(t'-t)]/\hbar}\langle V^2_{\delta\mathbf{p},\omega}\rangle, \tag{51a}$$

$$\propto \int d\omega J(\omega)\exp[i2\omega(t'-t)/\hbar] \times \mathrm{Re}\left\{\int_{\hbar/L}^{p_F} d\delta p_\perp \frac{\exp[i\delta p_\perp \delta r_\perp/\hbar]}{[\delta p_\perp^2 + (\omega/v_F)^2]^{1/2}}\right\}. \tag{51b}$$

Here, $\delta\mathbf{r}(t',t)=[\mathbf{r}_{\gamma'}(t')-\mathbf{r}_\gamma(t)]$. To get the second line, we wrote $\delta\mathbf{r}(t',t)=(\delta r_\parallel, \delta r_\perp)$ in the basis parallel and perpendicular to $\mathbf{p}$, we then inserted Eq. (50), evaluated the $\delta p_\parallel$ integral, and noted that $\delta r_\parallel = v_F(t'-t)$. Equation (51) expresses the correlator of the Coulomb interaction along classical trajectories in the form convenient for our semiclassical approach, Eq. (46). At first sight, the form of the interaction in Eqs. (49) and (50) does not appear to correspond to a classical-noise field since it is a function of the momentum, $\mathbf{p}_\gamma(t)$, of *system* paths. The correlator must, however, be evaluated on weak-localization loops, in which case one can use the fact that $r_{\parallel\gamma'}(t)=r_{\parallel\gamma}(t)=v_Ft$ throughout the encounter region to perform the Fourier transform. Thus, the interaction term in Eq. (51b) is equivalent to a classical-noise field which is a single function of $\delta\mathbf{r}$ and t for all $\mathbf{p}_\gamma$. This function must simply be chosen such that the integral over $\delta p_\parallel$ reduces to Eq. (51b).

The time-dependent part of the correlator is given by the ω integral in Eq. (51b). We assume that the temperature is high enough, $k_BT > \hbar v_F/L$, that the correlation time becomes shorter than the time of flight L/v_F through the cavity. Accordingly, we treat the noise as δ correlated in time and set $t'=t$ from now on.

We next investigate the properties of the real part of the $\delta p_\perp$ integral in Eq. (51b), giving the spatial dependence of the correlator. We write it as

$$G(\delta r_\perp) = \mathrm{Re}\left\{\int_{\delta r_\perp/L}^{p_F\delta r_\perp/\hbar} \frac{dxe^{ix}}{[x^2 + (\delta r_\perp/L_\omega)^2]^{1/2}}\right\}, \tag{52}$$

where $L_\omega = \hbar v_F/\omega$ is the distance a system particle will travel on the time scale that the ω-energy component of the noise fluctuates. For the ballistic model of the e-e interactions to be valid, we need that $L_\omega \ll L$, but we assume that $L_\omega \gg \lambda_F$. We can easily evaluate this integral in the following regimes:[78]

$$G(\delta r_\perp) \simeq \begin{cases} \ln[L_\omega/\lambda_F] & \text{for } \delta r_\perp \ll \lambda_F \\ \ln[L_\omega/\delta r_\perp] & \text{for } \lambda_F \ll \delta r_\perp \ll L_\omega \\ 0 & \text{for } L_\omega \ll \delta r_\perp \sim L, \end{cases} \tag{53}$$

where we neglected all $\mathcal{O}[1]$ terms (for example, the result for $\delta r_\perp \gg L_\omega$ is actually $\mathcal{O}[L_\omega/\delta r_\perp] \lesssim \mathcal{O}[1]$). The crossover between these regimes is smooth. We thus conclude that $K_{\mathrm{noise}}(x)$, as defined by Eq. (46), becomes

$$K_{\mathrm{noise}}(\delta r/L_\omega) = \frac{\ln[L_\omega/\delta r_\perp]}{\ln[L_\omega/\lambda_F]}. \tag{54}$$

This function does *not* decay fast as $\delta r_\perp$ grows, and thus it *cannot* be treated in the manner we do elsewhere in this paper, i.e., we cannot write an equation analogous to Eq. (26). Instead, we note that the dephasing rate in the vicinity of the encounter (where $\lambda_F \ll \delta r_\perp \ll L_\omega$) goes like $[G(0) - G(\lambda_F \ll \delta r_\perp \ll L_\omega)] = \ln[\delta r_\perp/\lambda_F]$, while the dephasing rate in the loop, τ_ϕ^{-1}, goes like $[G(0) - G(\delta r_\perp \sim L_\omega)] \sim \ln[L_\omega/\lambda_F]$. Now, we note that the integral over ω is dominated by $\omega \simeq k_BT \ll E_F$; thus, we can define $L_T = \hbar v_F/k_BT$ and write $\ln[L_\omega/\lambda_F] = \ln[L_T/\lambda_F] - \ln[\hbar\omega/k_BT]$. We can neglect the second term as it is much smaller than the first and thereby replace L_ω with L_T in the above formulas. In this way, we reproduce the result in Ref. 24 that the dephasing rate in the vicinity of the encounter is

$$\tilde{\tau}_\phi^{-1}(\delta r_\perp \ll L_T) = \tau_\phi^{-1}\frac{\ln[\delta r_\perp/\lambda_F]}{\ln[L_T/\lambda_F]}, \tag{55}$$

while $\tilde{\tau}_\phi^{-1}(\delta r_\perp \gtrsim L_T) = \tau_\phi^{-1}$. This is rather different from the systems considered elsewhere in this paper where the dephasing rate is approximately zero for $\delta r_\perp < \xi$ and approximately constant for $\delta r_\perp > \xi$.

We now calculate the effect of such a $\delta r_\perp$-dependent dephasing rate. We note that close to the encounter, $\delta r_\perp = \frac{1}{2}\epsilon L e^{\lambda\tau}$, where τ is the time measured from the encounter. We split the dephasing into two contributions. The first contribution is where $\delta r_\perp \geq L_T$ (here, dephasing is time independent, at the rate τ_ϕ^{-1}), and the second is where the paths have $\lambda_F < \delta r_\perp < L_T$ (here, dephasing is time dependent). The boundary between the two contributions is at $\tau = T_T(\epsilon)/2$, where we define $T_T(\epsilon) = \lambda^{-1}\ln[L_T^2/(L\epsilon)^2]$. The lower bound on the second contribution ($\delta r_\perp = \lambda_F$) is at time $\tau = T_T(\epsilon)/2 - \lambda^{-1}\ln[L_T/\lambda_F]$. Then, the exponent induced by the dephasing is

$$-\frac{t_2-t_1-T_T(\epsilon)}{\tau_\phi}-2\int_{T_T/2-\lambda^{-1}\ln[L_T/\lambda_F]}^{T_T/2}\frac{d\tau}{\tilde{\tau}_\phi(\delta r_\perp)}$$
$$=-\frac{t_2-t_1-T_T(\epsilon)}{\tau_\phi}-\frac{\lambda^{-1}\ln[L_T/\lambda_F]}{\tau_\phi}, \quad (56)$$

where to evaluate the integral, we defined $\tau'=\tau-T_T(\epsilon)/2$. The first term (which comes from the dephasing in the loop) alone would give no exponential term in the dephasing. The integral of that term over t_2-t_1 gives it a form $T_L(\epsilon)-T_T(\epsilon)=\tau_{L_T}$ giving an exponent like in Eq. (31) with $\xi=L_T$. However, we also have the second term which gives dephasing in the vicinity of the encounter; we can write it in terms of an Ehrenfest time using $\lambda^{-1}\ln[L_T/\lambda_F]=\tau_E^{\rm cl}-\frac{1}{2}\tau_{L_T}$. Summing the two terms, we find that the exponential term in the dephasing goes like $\tilde{\tau}/\tau_\phi$, with $\tilde{\tau}=\tau_E^{\rm cl}+\frac{1}{2}\tau_{L_T}$. This is the result which we gave in Eq. (57) and was found in Ref. 24 (neglecting the τ_{L_T} term).

Because λ_F is the scale of Friedel oscillations, one might have expected that electron-electron interactions give a noise with a correlation length $\xi\sim\lambda_F$, which would lead to a suppression $\propto\exp[-2\tau_E^{\rm cl}/\tau_\phi]$ of weak localization, instead of $\exp[-\tau_E^{\rm cl}/\tau_\phi]$. The factor of 2 difference between the correct result and this naive argument is due to the fact that all scales (i.e., all values of δp) contribute to the noise induced by the electron-electron interactions.

B. Noise due to the coupling to the electrostatic environment

Our aim here is to show that electron-electron interactions do *not* automatically lead to dephasing, which is an exponential function of the Ehrenfest time. It only happens when the q integral is divergent at its upper limit, with an upper cutoff of order p_F. If the q integral is cut off by some other length scale, then the dephasing of weak localization will be independent of the Ehrenfest time.

The example we consider is noise in a two-dimensional system due to electron-electron interactions between the system and the gates. A typical experimental setup is sketched in Fig. 6. The gates are bulk metal; the electrons in the system will feel fluctuations of electrons at the surface of the gates. One can expect that these fluctuations at the surface of the gate are sufficiently well confined to two dimensions (by screening in the bulk of the gate) that they will cause a noise field in the system of a form similar to Eq. (49). However, the fact that the distance between the gates and the chaotic system is D means that the natural upper cutoff on the q integral will be $\hbar/D$ and not p_F. Assuming $D\ll L,L_\omega$, we replace p_F by $\hbar/D$ throughout the derivation in Sec. III A, and find that

$$g_{\rm gate\ e\text{-}e}^{\rm wl}=\frac{g_0^{\rm wl}}{1+\tau_D/\tau_\phi}\exp[-\tau_\xi/\tau_\phi], \quad (57)$$

with $\xi=(L_TD)^{1/2}$ and hence $\tau_\xi=\lambda^{-1}\ln[L^2/(L_TD)]$. The dephasing rate here is $\tau_\phi^{-1}\propto D^{-1}$. In systems in which dephasing is dominated by thermal system-gate interactions, we therefore expect a dephasing that is τ_E independent and algebraic in τ_ϕ for $D\sim L$.

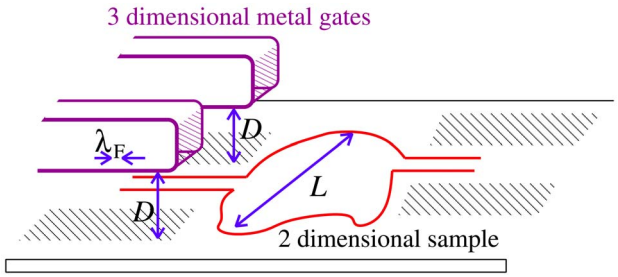

FIG. 6. (Color online) Sketch of a typical chaotic quantum dot in a two-dimensional electron gas (2DEG). The dot is defined by metallic gates which are biased to deplete the 2DEG everywhere except in the regions defining the leads and the dot. These gates are a distance D above the 2DEG (with $D\gg\lambda_F^{\rm gate}$). At finite temperature, the electrons at the surface of these metallic gates will fluctuate, leading to noise which will be felt by the electrons in the chaotic quantum dot.

In real experiments, the gates are typically much more disordered than the chaotic system; thus, we can easily have a situation in which the thermally excited modes in the gates are diffusive—or even localized by a charge trap at the edge of a gate—in which case their noise field will be similar to that in Refs. 8 and 9. This modifies the integrand of the q integral; however, the upper cutoff will still be $\hbar/D$, and therefore dephasing will again be τ_E independent.

In general, dephasing is due to a combination of e-e interactions *within* the system and the Coulomb coupling between the system and external charge distributions in gates and other reservoirs of charges. Which of these sources of dephasing dominates is determined by microscopic details which we do not discuss here, in particular, the temperatures and mean free paths of both system and gates.[13]

IV. DEPHASING-LEAD MODEL

In its simplest formulation, the dephasing-lead model consists of adding a fictitious lead 3 to the cavity. This is illustrated in Fig. 7. Contrary to the two real leads L, R, the potential voltage on lead 3 is tuned such that the net current through it is zero. Every electron that leaves through lead 3 is replaced by one with an unrelated phase, leading to a loss of phase information without loss of current.

In this situation, the conductance from L to R is given by[16]

$$g=T_{RL}+\frac{T_{R3}T_{3L}}{T_{3L}+T_{3R}}, \quad (58)$$

where T_{nm} is the conductance from lead m to lead n in the absence of a voltage on lead 3. We separate the Drude and weak-localization parts of T_{nm},

$$T_{nm}=T_{nm}^D+\delta T_{nm}+\mathcal{O}[N_T^{-1}], \quad (59)$$

where the Drude contribution T_{nm}^D is $\mathcal{O}[N_T]$ and the weak-localization contribution δT_{nm} is $\mathcal{O}[N_T^0]$ and $N_T=N_L+N_R+N_3$ is the total number of channels in this three-terminal

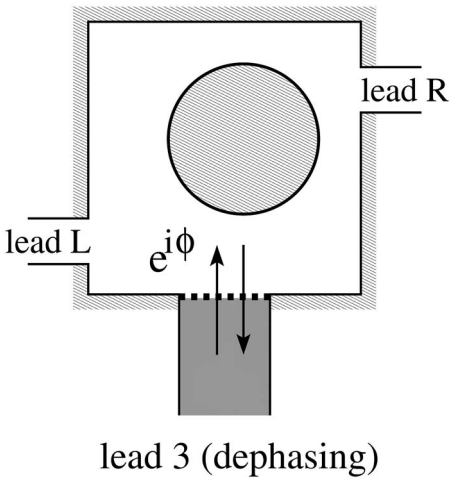

FIG. 7. Schematic of the dephasing-lead model. The system is an open quantum dot with an extra lead (lead 3), whose voltage is chosen to make a zero current flow (on average) in that lead. This extra lead thereby causes dephasing without loss of particles.

geometry. We expand g for large N_T and collect all $\mathcal{O}[N_T]$ terms (Drude contributions) and all $\mathcal{O}[N_T^0]$ terms (weak-localization contributions) to get $g=g^D+g^{\rm wl}$ with

$$g^D = T^D_{RL} + \frac{T^D_{R3}T^D_{3L}}{T^D_{3L}+T^D_{3R}}, \tag{60a}$$

$$g^{\rm wl} = \delta T_{RL} + \frac{(T^D_{R3})^2\delta T_{3L} + (T^D_{3L})^2\delta T_{3R}}{(T^D_{3R}+T^D_{3L})^2}. \tag{60b}$$

These equations form the basis of our semiclassical derivation of weak localization in the dephasing-lead model. We first consider the case of a dephasing lead perfectly coupled to the cavity, and then move on to consider a dephasing lead with a tunnel barrier of transparency $\rho<1$. We finally discuss multiple dephasing leads.

A. Dephasing lead without tunnel barrier

1. Weak localization

The Drude conductance and weak-localization correction from lead m to lead n in a three-lead cavity are

$$T^D_{nm} = \frac{N_nN_m}{N_T}, \tag{61}$$

$$\delta T_{nm} = -\frac{N_nN_m}{N_T^2}\exp[-\tau_E^{\rm cl}/\tilde{\tau}_D], \tag{62}$$

where $\tilde{\tau}_D^{-1}=(\tau_0 L)^{-1}(W_L+W_R+W_3)$, in terms of τ_0, the time of flight across the system. We substitute these results into Eqs. (60a) and (60b) and write the answer in terms of the dwell time in the two-lead (L and R) geometry, τ_D, and the dephasing rate, τ_ϕ^{-1}, which we define as the decay rate to lead 3,

$$\tau_D^{-1} = (\tau_0 L)^{-1}(W_L+W_R), \tag{63}$$

$$\tau_\phi^{-1} = (\tau_0 L)^{-1}W_3. \tag{64}$$

We have $\tilde{\tau}_D^{-1}=\tau_D^{-1}+\tau_\phi^{-1}$ and, from this, we find the Drude conductance and weak-localization correction,

$$g^D = g_0^D, \tag{65}$$

$$g^{\rm wl} = \frac{g_0^{\rm wl}}{1+\tau_D/\tau_\phi}\exp[-\tau_E^{\rm cl}/\tau_\phi]. \tag{66}$$

Here, g_0^D and $g_0^{\rm wl}$ are the results for a two-lead cavity in the absence of dephasing, Eqs. (17) and (32).

The weak-localization correction with a dephasing lead has a similar structure to that with a real environment. However, here, the time scale involved in the additional exponential suppression contains no independent parameter analogous to ξ. We could have expected that the width of the dephasing lead would play a role similar to ξ. However, this turns out not to be the case; instead, the Fermi wavelength appears in place of ξ, so the time scale in the additional exponential suppression is the Ehrenfest time $\tau_E^{\rm cl}$.

2. Universal conductance fluctuations

In the absence of tunnel barrier, we can go further and calculate conductance fluctuations at almost no extra cost. From Eqs. (58) and (59), we get the following expression for the variance of the conductance to order $\mathcal{O}[N_T^0]$:

$$\begin{aligned}\text{var } g = \text{var } T_{RL} &+ \frac{(T^D_{3R})^4\ \text{var } T_{3L} + (T^D_{3L})^4\ \text{var } T_{3R}}{(T^D_{3R}+T^D_{3L})^4} \\ &+ 2\frac{(T^D_{3R}T^D_{3L})^2\ \text{covar}(T_{3L},T_{3R})}{(T^D_{3R}+T^D_{3L})^4} \\ &+ 2\frac{(T^D_{3L})^2\ \text{covar}(T_{RL},T_{3R})}{(T^D_{3R}+T^D_{3L})^2} + 2\frac{(T^D_{3R})^2\ \text{covar}(T_{RL},T_{3L})}{(T^D_{3R}+T^D_{3L})^2}.\end{aligned} \tag{67}$$

In the universal regime, Ref. 10 gives, to order $\mathcal{O}[N_T^0]$ in the presence of time-reversal symmetry,

$$\text{var } T_{ij} = \frac{N_i^2N_j^2}{N_T^4}, \tag{68}$$

$$\text{covar}(T_{ij},T_{ik}) = \frac{N_i^2N_jN_k}{N_T^4}. \tag{69}$$

Reference 53 showed that Eq. (68) remains valid even at finite τ_E/τ_D. Inspection of their calculation for var T_{ij} shows that the same conclusion also applies to covar(T_{ij},T_{ik}), and thus Eq. (69) still holds independently of τ_E/τ_D. Together with Eq. (63), this straightforwardly leads to

$$\text{var } g = \frac{N_R^2N_L^2}{(N_R+N_L)^4}\frac{1}{(1+\tau_D/\tau_\phi)^2}. \tag{70}$$

In the universal regime, this result was previously derived in Ref. 11. We thus conclude that, in the dephasing-lead model without tunnel barrier, conductance fluctuations exhibit the universal behavior of Eq. (70). Below, we confirm this result numerically.

B. Dephasing lead with tunnel barrier

Putting a tunnel barrier on the dephasing lead 3 is attractive because one can avoid the local character of the dephasing-lead model by considering a wide third lead with an almost opaque barrier.[11] Additionally, this is the model studied numerically in Ref. 23 in the context of conductance fluctuations. Weak localization and shot noise in this model have been considered within the trajectory-based semiclassical approach in Ref. 56, and here we only mention the main results.

According to Ref. 56, when all leads are connected to the cavity via tunnel barriers, with the barrier on lead m having transparency $\rho_m \in [0,1]$, the Drude conductance between leads m and n, T^D_{nm}, and the weak-localization correction δT_{nm} are

$$T^D_{nm} = \rho_n \rho_m N_n N_m / \mathcal{N}, \tag{71}$$

$$\delta T_{nm} = \rho_n \rho_m \frac{N_n N_m}{\mathcal{N}^2}\left(\rho_n + \rho_m - \frac{\tilde{\mathcal{N}}}{\mathcal{N}}\right) \times \exp[-\tau_E^{\mathrm{op}}/\tau_{D_2} - (\tau_E^{\mathrm{cl}} - \tau_E^{\mathrm{op}})/\tau_{D_1}]. \tag{72}$$

Here, $\tau_{D1}^{-1} = (\tau_0 L)^{-1} \Sigma_n \rho_n W_n$ and $\tau_{D2}^{-1} = (\tau_0 L)^{-1} \Sigma_n \rho_n (2-\rho_n) W_n$ are the single path and the paired path survival times, respectively, W_n is the width of lead n, $\mathcal{N} = \Sigma_k \rho_k N_k$, and $\tilde{\mathcal{N}} = \Sigma_k \rho_k^2 N_k$.

Now, we assume that $\rho_L = \rho_R = 1$ so only the dephasing lead has a tunnel barrier. Substituting the Drude and weak-localization contributions into Eq. (60b), we find that

$$g^{\mathrm{wl}} = \frac{g_0^{\mathrm{wl}}}{1 + \tau_{D1}/\tau_\phi} \exp[-(1-\rho)\tau_E^{\mathrm{op}}/\tau_\phi - \tau_E^{\mathrm{cl}}/\tau_\phi]. \tag{73}$$

The argument in the exponent in Eq. (73) has a simple physical meaning. It is the probability that a path survives throughout the paired region ($\tau_E^{\mathrm{op}}/2$ on either side of the encounter) without escaping into lead 3, multiplied by the probability to survive the extra time ($\tau_E^{\mathrm{cl}} - \tau_E^{\mathrm{op}}$) unpaired without escaping into lead 3 (to close a loop of length τ_E^{cl}). The first probability is $\exp[-(2-\rho)\tau_E^{\mathrm{op}}/\tau_\phi]$, while the second is $\exp[-(\tau_E^{\mathrm{cl}} - \tau_E^{\mathrm{op}})/\tau_\phi]$.

We note that if we consider a nearly opaque barrier, the relevant time scale involved in the exponent is $\tau_E^{\mathrm{cl}} + \tau_E^{\mathrm{op}} \simeq 2\tau_E^{\mathrm{cl}}$. Thus, by tuning the opacity of the barrier, we can vary the exponential contribution to dephasing from $\exp[-\tau_E^{\mathrm{cl}}/\tau_\phi]$ to $\exp[-2\tau_E^{\mathrm{cl}}/\tau_\phi]$, but we cannot remove the exponent. In particular, we cannot mimic dephasing due to a real environment with $\xi \sim L$, Eq. (31), since it has only a power-law dephasing.

There is to date no theory for conductance fluctuations at finite Ehrenfest time in the presence of tunnel barriers, and constructing such a theory would require a formidable theoretical endeavor. Numerically, Ref. 23 observed that, in contrast to the dephasing-lead model without tunnel barrier, conductance fluctuations in the presence of a dephasing lead with a tunnel barrier are exponentially damped $\propto \exp[-\tau_E/\tau_\phi]$.

C. Multiple dephasing leads

The n probe dephasing model consists of adding n fictitious leads to the cavity (labeled $\{3,\ldots,n+2\}$) in addition to leads L, R. The voltage on each supplementary lead is tuned so that the current it carries is zero. Without loss of generality, we defined $V_R = 0$, then we get the set of equations

$$I_R = T_{RL} V_L + \mathbf{T}_R^T \mathbf{V}, \tag{74a}$$

$$0 = \mathbf{I} = -\mathbf{T}_{\mathrm{sub}} \mathbf{V} + \mathbf{T}_L V_L, \tag{74b}$$

where the superscript T indicates the transpose. The column vectors $\mathbf{I}$, $\mathbf{V}$ have an ith element given by the current or voltage, respectively, for the dephasing lead $i \in \{3, n+2\}$. The column vectors $\mathbf{T}_L$ and $\mathbf{T}_R$ have an ith element given by $\mathbf{T}_{Li}$ and $\mathbf{T}_{Ri}$, respectively. Finally, $\mathbf{T}_{\mathrm{sub}}$ has matrix elements given by

$$[\mathbf{T}_{\mathrm{sub}}]_{ij} = N_i \delta_{ij} - T_{ij}, \tag{75}$$

$$= \left[\sum_{k \neq j} T_{kj}\right] \delta_{ij} - T_{ij}(1 - \delta_{ij}), \tag{76}$$

where again $i,j \in \{3, n+2\}$. Substituting $\mathbf{V}$ from Eq. (74b) into Eq. (74a) and using $I_R = g V_L$ give us the conductance from L to R as

$$g = T_{LR} + \mathbf{T}_L^T \mathbf{T}_{\mathrm{sub}}^{-1} \mathbf{T}_R. \tag{77}$$

Thus, finding g requires the inversion of $\mathbf{T}_{\mathrm{sub}}$. This is cumbersome, so instead we present a simple argument to extract only the information we are interested in—the nature of the exponential in the dephasing.

We argue that whatever the formula for conductance for n dephasing leads is, we can expand it in powers of N and collect the $\mathcal{O}[N^0]$ terms to get a formula for weak localization of the form

$$g^{\mathrm{wl}} = \delta T_{LR} + \sum_{j=3}^{n+2} A_j \delta T_{Lj} + B_j \delta T_{jR} + \sum_{i,j=3}^{n+2} C_{ij} \delta T_{ij}. \tag{78}$$

Here, the sum is over all dephasing leads. To get the prefactors A_j, B_j, C_{ij}, we would have to solve the full problem by inverting $\mathbf{T}_{\mathrm{sub}}$; however, we can already see that, to leading order, they are combinations of Drude conductances and thus independent of the Ehrenfest time. In contrast, all the weak-localization contributions contain an exponential of the form [τ_{D_1} and τ_{D_2} are defined below Eq. (72)]

$$\exp[-\tau_E^{\mathrm{op}}/\tau_{D_2} + (\tau_E^{\mathrm{cl}} - \tau_E^{\mathrm{op}})/\tau_{D_1}]. \tag{79}$$

Thus, defining τ_ϕ^{-1} as the rate of escaping into any of the dephasing leads, so $\tau_\phi^{-1} = (\tau_0 L)^{-1} \Sigma_{j=3}^n \rho_j W_j$, we see that g^{wl} decays with an exponential

$$g^{\mathrm{wl}} \propto \exp[-(1-\tilde{\rho})\tau_E^{\mathrm{op}}/\tau_\phi - \tau_E^{\mathrm{cl}}/\tau_\phi], \tag{80}$$

where we define $\tilde{\rho}$ such that $\tilde{\rho}\tau_\phi^{-1} = (\tau_0 L)^{-1} \Sigma_j \rho_j^2 W_j$. We have just shown that multiple dephasing leads cause an exponential suppression of the weak localization which is qualitatively similar to that caused by a single dephasing lead. The exponent is proportional to the Ehrenfest time and contains no independent parameter analogous to ξ.

V. NUMERICAL SIMULATIONS

A. Open kicked rotators

Because of the slow, logarithmic increase of τ_E with the size M of the Hilbert space, the ergodic semiclassical regime $\tau_E \gtrsim \tau_D$, $\lambda\tau_D \gg 1$ is unattainable by standard numerical methods. We therefore follow Refs. 23, 44, 48, 51, 52, and 79 and consider the open kicked rotator model.

1. Dephasing-lead model

The system is described by the time-dependent Hamiltonian

$$H = \frac{(p-p_0)^2}{2} + K\cos(x-x_0)\sum_n \delta(t-n\tau_0). \tag{81}$$

The kicking strength K drives the dynamics from integrable ($K=0$) to fully chaotic ($K \gtrsim 7$). The Lyapunov exponent in the classical version of the kicked rotator is given by $\lambda\tau_0 \approx \ln(K/2)$. In most quantum simulations, however, one observes an effective Lyapunov exponent λ_{eff} instead that is systematically smaller than λ by as much as 30%.[80] Two parameters, p_0 and x_0, are introduced to break two parities and drive the crossover from the $\beta=1$ to the $\beta=2$ universality class,[37] corresponding to breaking the time-reversal symmetry.

We quantize the Hamiltonian of Eq. (81) on the torus $x,p \in [0,2\pi]$, by discretizing the momentum coordinates as $p_l = 2\pi l/M$, $l=1,\ldots,M$. A quantum representation of the Hamiltonian of Eq. (81) is provided by the unitary $M\times M$ Floquet operator U, which gives the time evolution for one iteration of the map. For our specific choice of the kicked rotator, the Floquet operator has matrix elements

$$U_{l,l'} = M^{-1/2} e^{-(\pi i/2M)[(l-l_0)^2+(l'-l_0)^2]} \times \sum_m e^{2\pi i m(l-l')/M} e^{-(iMK/2\pi)\cos[2\pi(m-m_0)/M]}, \tag{82}$$

with $l_0 = p_0 M/2\pi$ and $m_0 = x_0 M/2\pi$. The Hilbert space size M is given by the ratio L/λ_F of the linear system size to the Fermi wavelength.

To investigate transport, we open the system by defining $n+2 \geq 2$ contacts to leads via absorbing phase-space strips $[l_i - N_i/2, l_i + N_i/2 - 1]$, $i=1,2,\ldots,n+2$. With $N_T = \Sigma_i N_i$, we construct an $N_T \times N_T$ scattering matrix from the Floquet operator U as[81]

$$S(\varepsilon) = \sqrt{\mathcal{J} - \mathcal{P}\mathcal{P}^\dagger} - \mathcal{P}\left[e^{-i\varepsilon}\mathcal{J} - U\sqrt{\mathcal{J} - \mathcal{P}^\dagger\mathcal{P}}\right]^{-1} U\mathcal{P}^\dagger. \tag{83}$$

The $N_T \times M$ projection matrix $\mathcal{P}$, which describes the coupling to the leads, has matrix elements

$$\mathcal{P}_{l,m} = \begin{cases} \gamma_l \delta_{lm} & \text{if } l \in \cup_i \{l^{(i)}\} \\ 0 & \text{otherwise,} \end{cases} \tag{84}$$

where $|\gamma_l|^2 = \rho_l \in [0,1]$ gives the transparency of the contact to the external channel l and $\cup_i \{l^i\}$ denotes the ensemble of cavity modes coupled to the external leads. Below, we focus on perfectly transparent contacts, $\rho_l = \gamma_l = 1$, $\forall l$.

The conductance [Eq. (60a)] in the dephasing-lead model is obtained from Eq. (83) with $n+2=3$ leads. The transport leads carry $N = N_L = N_R$ channels, which defines the dwell time through the system as $\tau_D/\tau_0 = M/2N$. The dephasing time $\tau_\phi/\tau_0 = M/N_3$ is defined by the number N_3 of channels carried by the third, dephasing lead, and the Ehrenfest time is given by

$$\tau_E^{\text{cl}} = \lambda^{-1}[\ln M + \mathcal{O}(1)]. \tag{85}$$

2. Open kicked rotator coupled to an environment

We extend the kicked rotator model to account for the coupling to external degrees of freedom. The exponential increase of memory size with number of particles forces us to focus on an environment modeled by a single chaotic particle. Therefore, we follow Ref. 67 and consider two coupled kicked rotators (with i=sys, env)

$$\mathcal{H} = H_{\text{sys}} + H_{\text{env}} + \mathcal{U},$$

$$H_i = \frac{(p_i - p_0)^2}{2} + K_i\cos(x_i - x_0)\sum_n \delta(t - n\tau_0),$$

$$\mathcal{U} = \varepsilon\,\sin(x_{sys} - x_{\text{env}} - 0.33)\sum_n \delta(t - n\tau_0). \tag{86}$$

In this model, the interaction potential $\mathcal{U}$ acts at the same time as the kicks, which facilitates the construction of the S matrix. For this particular choice of interaction, the correlation length $\xi = L$ so that one expects a universal behavior of dephasing, as in Eq. (1). The quantum representation of the coupled Hamiltonian is a unitary $(M_{\text{sys}}M_{\text{env}}) \times (M_{\text{sys}}M_{\text{env}})$ Floquet operator. We open the system (and not the environment) to two external leads by means of extended projectors $\mathbb{P}_{\text{tot}} = P^{(\text{L})} \otimes \mathbb{I}_{\text{env}} + P^{(\text{R})} \otimes \mathbb{I}_{\text{env}}$. A straightforward generalization of Eq. (83) defines an $(N_T M_{\text{env}}) \times (N_T M_{\text{env}})$ extended scattering matrix, from which we evaluate the conductance via Eq. (A11). We focus on the symmetric situation where the two leads carry the same number N of channels and average our data over a set of pure but random initial environment density matrices $\eta_{\text{env}}(\mathbf{q},\mathbf{q}';t=0)$. We estimate the dephasing time from the ε-induced broadening of two-particle levels in the corresponding closed two-particle kicked rotator, $\tau_\phi^{-1} = 0.43(\varepsilon/\hbar_{\text{eff}})^2$, with $\hbar_{\text{eff}} = 2\pi/M$ the effective Planck constant.[67]

B. Weak localization with dephasing

To investigate weak localization, we follow the same procedure as in Ref. 82 of taking a constant nonzero p_0, while varying x_0 (which hence plays the role of a magnetic field). The obtained magnetoconductance in the absence of dephasing is Lorentzian,[45,82]

$$g^{\text{wl}}(\Phi) = \frac{g^{\text{wl}}(0)}{1 + (m_0/m_c)^2}, \tag{87}$$

with $m_c = 4\pi/K\sqrt{M\tau_D}$. In Fig. 8, we compare the suppression of weak localization for the system-environment kicked ro-

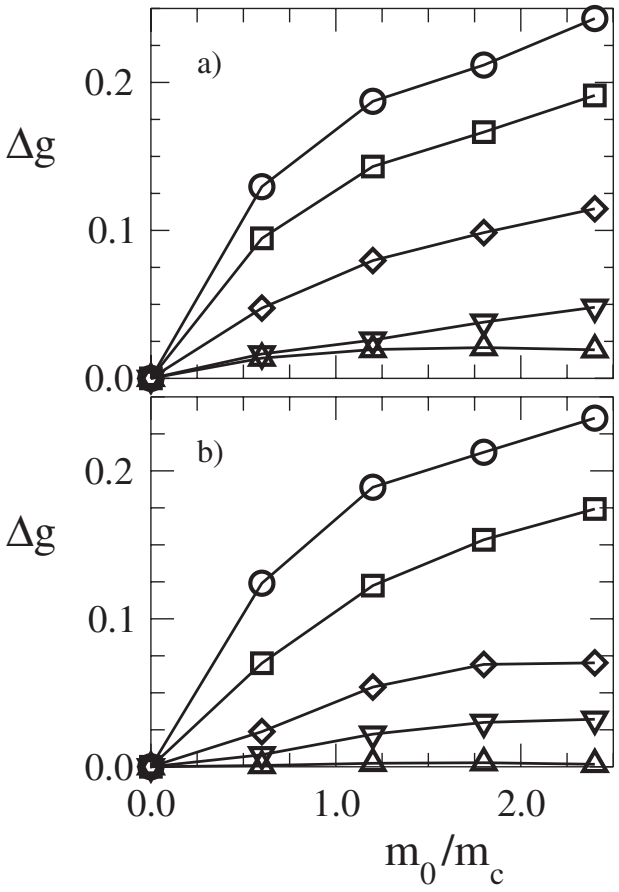

FIG. 8. (a) Magnetoconductance curves $\Delta g(x_0)=g(x_0)-g(0)$ for the double kicked rotator model (see text) with $K_{\rm sys}=K_{\rm env}=34.08$ ($\lambda_{\rm eff}\approx 2$), $\tau_D/\tau_0=8$, $\xi/L=1$, and Hilbert space sizes $M_{\rm sys}=256$, $M_{\rm env}=16$. Different symbols correspond to different dephasing times $\tau_\phi/\tau_D=\infty$ ($\hbar_{\rm eff}^{-1}\varepsilon=0$, circles), $\tau_\phi/\tau_D=4.8$ ($\hbar_{\rm eff}^{-1}\varepsilon\simeq 0.25$, squares), $\tau_\phi/\tau_D=1.2$ ($\hbar_{\rm eff}^{-1}\varepsilon\simeq 0.5$, diamonds), $\tau_\phi/\tau_D=0.3$ ($\hbar_{\rm eff}^{-1}\varepsilon\simeq 1$, downward triangles), and $\tau_\phi/\tau_D=0.07$ ($\hbar_{\rm eff}^{-1}\varepsilon\simeq 2$, upward triangles). Data are averaged over 25 different lead positions, each with 25 different quasienergies and 10 different initial environment states. (b) Magnetoconductance curves for the open kicked rotator with transparent dephasing lead (see text) with $K=34.08$, $\tau_D/\tau_0=8$, and Hilbert space size $M=256$. Different symbols correspond to different dephasing times $\tau_\phi/\tau_D=\infty$ (circles), $\tau_\phi/\tau_D=5$ (squares), $\tau_\phi/\tau_D=1.25$ (diamonds), $\tau_\phi/\tau_D=0.5$ (downward triangles), and $\tau_\phi/\tau_D=0.25$ (upward triangles). Data are averaged over 225 different lead positions, each with 50 different quasienergies.

tator [panel (a), top] and the dephasing-lead kicked rotator [panel (b), bottom]. For both models, we show five magnetoconductance curves, corresponding to five different ratios τ_ϕ/τ_D. All curves exhibit the expected Lorentzian behavior vs m_0/m_c; however, the amplitude of the magnetoconductance is reduced as τ_ϕ/τ_D is reduced. This allows one to extract the τ_ϕ dependence of $g^{\rm wl}$. For the system-environment model, we found no significant departure from our analytical prediction, Eq. (31) with $\tau_\xi=0$ [since the interaction in Eq. (86) has $\xi=L$]. The same behavior is observed for the dephasing-lead model, as long as τ_ϕ/τ_D is large; however, compared to the system-environment kicked

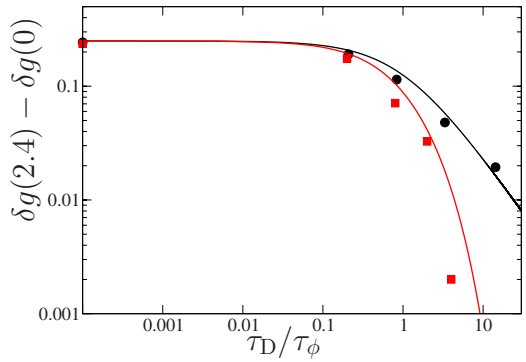

FIG. 9. (Color online) Amplitude $\delta g(m_0/m_c=2.4)-\delta g(m_0/m_c=0)$ of the weak-localization correction to the conductance as a function of τ_D/τ_ϕ for the double kicked rotator model (circles) and the open kicked rotator with transparent dephasing lead (squares). The black line gives the universal algebraic behavior $(1+\tau_D/\tau_\phi)^{-1}/4$, and the red line is a guide to the eyes, including an exponential decay with $\tau_E^{\rm cl}=2.78$, on top of the universal decay.

rotator, the damping of magnetoconductance accelerates as τ_ϕ/τ_E becomes comparable to or smaller than 1. When this regime is reached, magnetoconductance curves for the dephasing-lead model lies significantly below those of the system-environment model, even when the latter corresponds to shorter dephasing times (compare, in particular, the upward triangles in both panels of Fig. 8). This behavior is further illustrated in Fig. 9, where we plot the amplitude $\delta g(m_0/m_c=2.4)-\delta g(m_0/m_c)$ of the weak-localization corrections to the conductance as a function of τ_D/τ_ϕ. The data for the double kicked rotator nicely line up on the universal algebraic behavior $(1+\tau_D/\tau_\phi)^{-1}/4$ without any fitting parameter. This is clearly not the case for the dephasing-lead model, where an additional, exponential dependence on τ_ϕ emerges. We attribute this to the exponential damping factor $\propto\exp[-\tau_E/\tau_\phi]$ of Eq. (66). The data presented in Figs. 8 and 9 for $\tau_\phi^{-1}=0$ exhibit a weak dependence on $\exp[-\tau_E^{\rm cl}/\tau_D]$ only, with $\tau_E^{\rm cl}\lesssim 0.8$, which we attribute to terms of order 1 in Eq. (85).

All collected data (including some that we do not present here) thus confirm qualitatively—if not quantitatively—the validity of Eq. (66) for the dephasing-lead model.

C. Conductance fluctuations in the dephasing-lead model

Conductance fluctuations were studied numerically in Ref. 23 for the dephasing-lead model with a tunnel barrier of low transparency, and an exponential damping $\mathrm{var}(g)\propto\exp[-2\tau_E/\tau_\phi]$ was reported. Instead, here, we consider a model in which the dephasing lead is transparently coupled to the system. In Fig. 10, we show data for $\mathrm{var}(g)$ against τ_ϕ/τ_D, which is varied only by varying the width of the third, dephasing lead. There are four data sets (empty symbols) corresponding to a fixed classical configuration at different stages in the quantum-classical crossover, i.e., with increasing ratio $M=L/\lambda_F\in[128,8192]$. As M increases, so does τ_E/τ_ϕ; however, no change of behavior of $\mathrm{var}(g)$ is observed. These data are compared to a fifth set obtained in the univer-

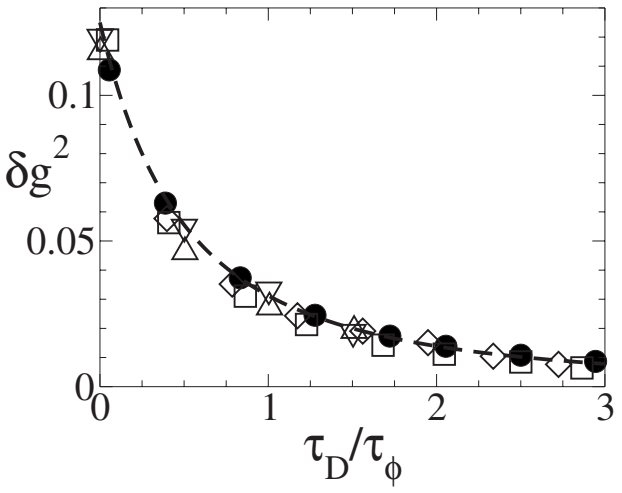

FIG. 10. Variance of the conductance vs τ_D/τ_ϕ for the open kicked rotator with $K=14$ and $\tau_D/\tau_0=5$ (empty symbols), transparently coupled to a dephasing lead. Different symbols correspond to different Hilbert space sizes (and hence different $\tau_E^{\rm cl}$) $M=128$ (squares, $\tau_E^{\rm cl}/\tau_D=0.6$), $M=512$ (diamonds, $\tau_E^{\rm cl}/\tau_D=0.75$), $M=2048$ (upward triangles, $\tau_E^{\rm cl}/\tau_D=0.9$), and $M=8192$ (downward triangles, $\tau_E^{\rm cl}/\tau_D=1.1$). Additional data for $K=144$, $\tau_D=25$, and $M=2048$ are also shown (full circles, $\tau_E^{\rm cl}/\tau_D=0.08$). The dashed line shows the universal behavior of Eq. (2). Unlike for weak localization (see Fig. 8) and for the dephasing-lead model with partial transparency (Ref. 48), the behavior of δg^2 remains universal and shows no noticeable dependence on $\tau_E^{\rm cl}/\tau_D$. Data are averaged over 50 different quasienergies and from 50 (for $N=8192$) to 500 (for $N=128$ and 512) different lead positions.

sal regime, $\tau_E/\tau_D \ll 1$, and the universal prediction of Eq. (70) (dashed line). These data confirm our analytical result, Eq. (70), that var(g) exhibits no Ehrenfest time dependence for the dephasing-lead model with perfectly transparent contacts.

VI. CONCLUSIONS

We have investigated the dephasing properties of open quantum chaotic system, focusing on the deep semiclassical limit where the Ehrenfest time is comparable to or larger than the dwell time through the system. We treated three models of dephasing. In the first one, the transport system is capacitively coupled to an external quantum chaotic system. For that model, we developed a scattering formalism, based on an extended scattering matrix $\mathbb{S}$, including the degrees of freedom of the environment. Transport properties are extracted from $\mathbb{S}$, once the environment has been traced out properly. In that model, we find that, in addition to the universal algebraic suppression $g^{\rm wl} \propto (1+\tau_D/\tau_\phi)^{-1}$ with the dwell time τ_D through the cavity and the dephasing rate τ_ϕ^{-1}, weak localization is exponentially suppressed by a factor $\propto \exp[-\tau_\xi/\tau_\phi]$, with a new time scale τ_ξ depending on the correlation length of the coupling potential between the system and the environment.

The second model we treated is that of dephasing due to a classical-noise field. We show that the new time scale τ_ξ plays the same role here as in the system-environment model. We then consider a classical Johnson-Nyquist noise model of electron-electron interactions. We show that $\xi \sim \lambda_F$ (and so τ_ξ equals the Ehrenfest time) when dephasing is dominated by electron-electron interactions within the system, but that $\xi \sim D$ when dephasing is dominated by interactions between electrons in the system and those in a gate, a distance D away.

The third model we treated is the dephasing-lead model. We found a similar exponential suppression of weak localization. To our surprise, however, it is the Fermi wavelength, not the dephasing-lead's width, which plays a role similar to ξ in that model. This inequivalence between the dephasing-lead model and dephasing due to a real environment or classical noise can be most clearly seen in a situation where the interaction with a real environment has $\xi \simeq L$. Then, the environment induces only power-law dephasing, which is impossible to mimic with a dephasing lead. For the dephasing-lead model, we also showed analytically and numerically that conductance fluctuations exhibit only power-law dephasing if the connection between the cavity and the dephasing lead is perfectly transparent. This is to be contrasted with the exponential dephasing observed for the dephasing-lead model with tunnel barrier and reflects the fact that the presence of tunnel barriers violates a sum rule, otherwise preserving the universality of conductance fluctuations vs τ_E/τ_D.[53]

Related results have been obtained for conductance fluctuations in Ref. 24, where different behaviors have been predicted for external sources—which give similar dephasing as our environment model—and internal source of dephasing—which qualitatively reproduce the prediction of Ref. 14.

ACKNOWLEDGMENTS

We thank I. Aleiner, P. Brouwer, M. Büttiker, and M. Polianski for useful and stimulating discussions. While working on this project, C.P. was supported by the Swiss National Science Foundation, which also funded the visits to Geneva of P.J. and R.W. P.J. expresses his gratitude to M. Büttiker and the Department of Theoretical Physics at the University of Geneva for their hospitality. This work was initiated in the summer of 2006 at the Aspen Center for Physics.

APPENDIX: SCATTERING APPROACH TO TRANSPORT IN THE PRESENCE OF AN ENVIRONMENT

Here, we extend the scattering approach to transport to account for those environmental degrees of freedom which couple to the system being studied. We follow the lines of the derivation of the expression for noise presented in Ref. 83, focusing on the two-terminal configuration. The following derivation is valid in the limit of pure dephasing, when there is no energy or momentum exchange between the system and environment.

1. Current operator and conductance

In the presence of an environment, the current operator at time t on a cross section deep inside of lead $\alpha=L,R$ (where

there is no system-environment interaction) reads

$$\hat{I}_\alpha(t) = \frac{e}{h}\int dE dE' e^{i(E-E')t/\hbar} \sum_{n\in\alpha} [\hat{a}^\dagger_{\alpha n}(E')\hat{a}_{\alpha n}(E) - \hat{b}^\dagger_{\alpha n}(E')\hat{b}_{\alpha n}(E)] \times \mathbb{I}_{\text{env}}. \tag{A1}$$

The second quantized operators $\hat{a}^{(\dagger)}$ and $\hat{b}^{(\dagger)}$ create and destroy incoming and outgoing system particles, respectively. Since the environment particles carry no current, the current operator acts as the identity operator $\mathbb{I}_{\text{env}}$ in the environment subspace. We could write $\mathbb{I}_{\text{env}}$ in terms of second quantized operators; however, for our present purpose, it is more convenient to write it as

$$\mathbb{I}_{\text{env}} = \int d\mathbf{q}|\mathbf{q}\rangle\langle\mathbf{q}|. \tag{A2}$$

As in Ref. 83, we now back evolve the outgoing states into incoming states, this time with an S matrix which also depends on the coordinates of the environment,

$$\hat{b}_{\alpha n}(E)\langle\mathbf{q}| = \sum_{\beta;j}\int d\mathbf{q}_0 \mathbb{S}_{\alpha\beta;nj}(\mathbf{q},\mathbf{q}_0;E,\tilde{E})\hat{a}_{\beta j}(\tilde{E})\langle\mathbf{q}_0|. \tag{A3}$$

Here, $\mathbb{S}_{\alpha\beta;nj}(\mathbf{q},\mathbf{q}_0;E,\tilde{E})$ gives the transmission amplitude from channel j in lead β with energy $\tilde{E}$ to channel n in lead α with energy E, while simultaneously, the environment evolves from $\mathbf{q}_0$ to $\mathbf{q}$. We can set $\tilde{E}=E$ because throughout this paper, we only consider the regime of pure dephasing. Using Eq. (A3), we rewrite the current operator as

$$\hat{I}_\alpha(t) = \frac{e}{h}\int d\mathbf{q}\int dE dE' e^{i(E-E')t/\hbar} \times \sum_n \Bigg\{ \hat{a}^\dagger_{\alpha n}(E')\hat{a}_{\alpha n}(E)\langle\Psi_{\text{env}}|\mathbf{q}\rangle\langle\mathbf{q}|\Psi_{\text{env}}\rangle - \int d\mathbf{q}_0' d\mathbf{q}_0 \sum_{\gamma,\beta}\sum_{jk} [\mathbb{S}_{\alpha\gamma;nj}(\mathbf{q},\mathbf{q}_0')]^\dagger \mathbb{S}_{\alpha\beta;nk}(\mathbf{q},\mathbf{q}_0) \times \hat{a}^\dagger_{\gamma j}(E')\hat{a}_{\beta k}(E)\langle\Psi_{\text{env}}|\mathbf{q}_0'\rangle\langle\mathbf{q}_0|\Psi_{\text{env}}\rangle \Bigg\}. \tag{A4}$$

We next rewrite the first line of Eq. (A4) as

$$\int d\mathbf{q}\sum_n \hat{a}^\dagger_{\alpha n}(E')\hat{a}_{\alpha n}(E)\langle\Psi_{\text{env}}|\mathbf{q}\rangle\langle\mathbf{q}|\Psi_{\text{env}}\rangle = \int d\mathbf{q}_0 d\mathbf{q}_0' \sum_{\gamma,\beta}\sum_{jk}\delta(\mathbf{q}_0'-\mathbf{q}_0)\delta_{\gamma\alpha}\delta_{\beta\alpha}\delta_{jk}\hat{a}^\dagger_{\gamma j}(E')\hat{a}_{\beta k}(E) \times \langle\Psi_{\text{env}}|\mathbf{q}_0'\rangle\langle\mathbf{q}_0|\Psi_{\text{env}}\rangle. \tag{A5}$$

Finally, we write the current operator in terms of the initial environment density matrix $\eta_{\text{env}}(\mathbf{q}_0,\mathbf{q}_0')=\langle\mathbf{q}_0|\Psi_{\text{env}}\rangle \times\langle\Psi_{\text{env}}|\mathbf{q}_0'\rangle$,

$$\hat{I}_\alpha(t) = \int d\mathbf{q}_0' d\mathbf{q}_0 \hat{I}^{(\text{red})}_\alpha(\mathbf{q}_0',\mathbf{q}_0;t)\,\eta_{\text{env}}(\mathbf{q}_0,\mathbf{q}_0'), \tag{A6}$$

where we defined the reduced current operator as

$$\hat{I}^{(\text{red})}_\alpha(\mathbf{q}_0',\mathbf{q}_0;t) = \frac{e}{h}\int d\mathbf{q}\int dE dE' e^{i(E-E')t/\hbar} \times \sum_{\gamma,\beta}\sum_{j,k} B^{jk}_{\gamma\beta}(\alpha,E,E';\mathbf{q}_0',\mathbf{q}_0)\hat{a}^\dagger_{\gamma j}(E')\hat{a}_{\beta k}(E), \tag{A7a}$$

$$B^{jk}_{\gamma\beta}(\alpha,E,E';\mathbf{q}_0',\mathbf{q}_0) = \delta(\mathbf{q}_0'-\mathbf{q}_0)\delta_{\gamma\alpha}\delta_{\beta\alpha}\delta_{jk} - \int d\mathbf{q}\sum_n [\mathbb{S}_{\alpha\gamma;nj}(\mathbf{q},\mathbf{q}_0')]^\dagger \mathbb{S}_{\alpha\beta;nk}(\mathbf{q},\mathbf{q}_0). \tag{A7b}$$

The current is obtained by taking the expectation value of the current operator over the system, using

$$\langle\langle \hat{a}^\dagger_{\gamma j}(E')\hat{a}_{\beta k}(E)\rangle\rangle = \delta_{\gamma\beta}\delta_{jk}\delta(E-E')f_\beta(E), \tag{A8}$$

where f_β is the Fermi function in lead β. The unitarity of $\mathbb{S}$ implies

$$\int d\mathbf{q}\sum_{\delta,n}[\mathbb{S}_{\delta\gamma;nj}(\mathbf{q},\mathbf{q}_0')]^\dagger \mathbb{S}_{\delta\beta;nk}(\mathbf{q},\mathbf{q}_0) = \delta(\mathbf{q}_0'-\mathbf{q}_0)\delta_{\beta\gamma}\delta_{jk}. \tag{A9}$$

We use this latter equality to rewrite the Kronecker δ's in Eq. (A8). Finally, the current in the left lead is

$$\langle\langle I_L\rangle\rangle = \frac{e}{h}\sum_{n,k}\int d\mathbf{q}_0' d\mathbf{q}_0 d\mathbf{q}\int dE[\mathbb{S}_{LR;nk}(\mathbf{q},\mathbf{q}_0')]^\dagger \mathbb{S}_{LR;nk}(\mathbf{q},\mathbf{q}_0) \times [f_L(E)-f_R(E)]\eta_{\text{env}}(\mathbf{q}_0,\mathbf{q}_0'). \tag{A10}$$

In the limit of zero temperature in the leads and assuming that the scattering matrix is not too strongly energy dependent, Eq. (A10) leads to the linear conductance

$$G = \frac{e^2}{h}\sum_{n,k}\int d\mathbf{q}_0' d\mathbf{q}_0 d\mathbf{q}[\mathbb{S}_{LR;nk}(\mathbf{q},\mathbf{q}_0')]^\dagger \mathbb{S}_{LR;kn}(\mathbf{q},\mathbf{q}_0) \times \eta_{\text{env}}(\mathbf{q}_0,\mathbf{q}_0'), \tag{A11}$$

with scattering matrices to be evaluated at the Fermi energy. From Eqs. (A10) and (A11), we see that both current and conductance are obtained by tracing over the environmental degrees of freedom of the square of the extended scattering matrix. Besides this prescription, these two equations are extremely similar to their counterpart in the standard scattering approach to transport. We also note that conductance fluctuations can be obtained by squaring Eqs. (A10) and (A11).

It is legitimate to expect that a complex environment—such as the chaotic system considered in this paper—has a complicated initial wave function, which, under ensemble averaging, is uncorrelated with itself on all scales greater than the environment wavelength. This justifies us treating the initial environment state as $\langle\eta_{\text{env}}(\mathbf{q}_0,\mathbf{q}_0')\rangle \sim (2\pi\hbar)^{Nd}\delta(\mathbf{q}_0-\mathbf{q}_0')/\Xi_{\text{env}}$.

2. Current noise

We follow similar steps as in the previous section to calculate the zero-frequency current noise. However, now, we have two current operators and hence two creation and two annihilation operators for the system.[83] The environment has two $\mathbb{I}_{\rm env}$ operators, each of which we write in the form $\int d\mathbf{q}|\mathbf{q}\rangle\langle\mathbf{q}|$ to get the current time correlator as

$$\langle\langle \hat{I}_\beta(t)\hat{I}_\alpha(0)\rangle\rangle = \left\langle\!\!\left\langle \int d\mathbf{q}_{03}d\mathbf{q}_{01}d\mathbf{q}'_{01}\hat{I}^{(\rm red)}_\beta(\mathbf{q}'_{01},\mathbf{q}_{03};t) \times \hat{I}^{(\rm red)}_\alpha(\mathbf{q}_{03},\mathbf{q}_{01};0)\,\eta_{\rm env}(\mathbf{q}_{01},\mathbf{q}'_{01})\right\rangle\!\!\right\rangle. \tag{A12}$$

The reduced current operator $\hat{I}^{(\rm red)}_\beta(\mathbf{q}',\mathbf{q};t)$ is given in Eq. (A7a). The zero-frequency noise power is obtained from the product of the deviations from the average current at times 0 and t. Consequently, it is proportional to

$$\int dt \int d\mathbf{q}_{03}d\mathbf{q}_{01}d\mathbf{q}'_{01}\langle\langle[\hat{I}^{(\rm red)}(\mathbf{q}'_{01},\mathbf{q}_{03};t) - \langle\langle\hat{I}^{(\rm red)}(\mathbf{q}'_{01},\mathbf{q}_{03};t)\rangle\rangle] \times[\hat{I}^{(\rm red)}(\mathbf{q}_{03},\mathbf{q}_{01};0) - \langle\langle\hat{I}^{(\rm red)}(\mathbf{q}_{03},\mathbf{q}_{01};0)\rangle\rangle]\rangle\rangle\,\eta_{\rm env}(\mathbf{q}_{01},\mathbf{q}'_{01}). \tag{A13}$$

There is only one trace over the environment here because we assume that we measure the current as a function of time in a given experiment (with a given initial $\eta_{\rm env}$), and then extract the average current (and the deviations from it) from that data set.

We need to take the following expectation value of products of creation and annihilation operators over the system[83]

$$\begin{aligned}&\langle\langle\hat{a}^\dagger_{\beta m}(E_2)\hat{a}_{\gamma n}(E_1)\hat{a}^\dagger_{\beta' m'}(E_4)\hat{a}_{\gamma' n'}(E_3)\rangle\rangle - \langle\langle\hat{a}^\dagger_{\beta m}(E_2)\hat{a}_{\gamma n}(E_1)\rangle\rangle \\ &\quad\times\langle\langle\hat{a}^\dagger_{\beta' m'}(E_4)\hat{a}_{\gamma' n'}(E_3)\rangle\rangle \\ &= \delta_{\beta\gamma'}\delta_{\gamma\beta'}\delta_{mn'}\delta_{nm'}\delta(E_2-E_3)\delta(E_1-E_4)f_\alpha(E_2) \\ &\quad\times[1\mp f_\beta(E_1)],\end{aligned} \tag{A14}$$

where the minus (plus) sign stands for fermions (bosons). From this, we finally get the zero-frequency noise power

$$\begin{aligned}S_{\alpha\alpha'}(0) = \frac{e^2}{h}\int dE \int d\mathbf{q}_{03}d\mathbf{q}_{01}d\mathbf{q}'_{01} &\times\sum_{\beta,\gamma}\sum_{m,n}B^{nm}_{\beta\gamma}(\alpha,E,E;\mathbf{q}'_{01},\mathbf{q}_{03})B^{mn}_{\gamma\beta}(\alpha',E,E;\mathbf{q}_{03},\mathbf{q}_{01}) \\ &\times\{f_\beta(E)[1\mp f_\gamma(E)]+[1\mp f_\alpha(E)]f_\beta(E)\} \\ &\times\eta_{\rm env}(\mathbf{q}_{01},\mathbf{q}'_{01}).\end{aligned} \tag{A15}$$

All the relevant information for shot noise is contained in the diagonal $S_{\alpha\alpha}$, $\alpha=L,R$. Shot noise is obtained by calculating this latter expression in the limit of low temperature but finite voltage bias V between the two leads. In that case, it is easily checked that the contribution to B arising from the first term on the right-hand side of Eq. (A7b) does not contribute, and one gets

$$\begin{aligned}S_{\alpha\alpha}(0) = \frac{e^2}{h}\int dE\sum_{\beta\neq\gamma}\int d\mathbf{q}_3d\mathbf{q}_1d\mathbf{q}_{03}d\mathbf{q}_{01}d\mathbf{q}'_{01} &\times\sum_{m,n}\sum_{m',n'}[\mathbb{S}_{\alpha\beta;m'm}(\mathbf{q}_3,\mathbf{q}'_{01};E)]^\dagger\mathbb{S}_{\alpha\gamma;m'n}(\mathbf{q}_3,\mathbf{q}_{03};E) \\ &\times[\mathbb{S}_{\alpha\gamma;n'n}(\mathbf{q}_1,\mathbf{q}_{03};E)]^\dagger\mathbb{S}_{\alpha\beta;n'm}(\mathbf{q}_1,\mathbf{q}_{01};E) \\ &\times\{f_\beta(E)[1\mp f_\gamma(E)]+[1\mp f_\alpha(E)]f_\beta(E)\} \\ &\times\eta_{\rm env}(\mathbf{q}_{01},\mathbf{q}'_{01}).\end{aligned} \tag{A16}$$

We finally assume a slow dependence of $\mathbb{S}$ on E, in which case the integral over the energy is easily performed, giving a factor eV. For a two-lead device (L, R), we find that

$$\begin{aligned}S_{RR}(0) = \frac{2e^3V}{h}\int d\mathbf{q}_3d\mathbf{q}_1d\mathbf{q}_{03}d\mathbf{q}_{01}d\mathbf{q}'_{01} &\times\sum_{m\in L}\sum_{n,m',n'\in R}[\mathbb{S}_{RL;m'm}(\mathbf{q}_3,\mathbf{q}'_{01};E)]^\dagger \\ &\times\mathbb{S}_{RR;m'n}(\mathbf{q}_3,\mathbf{q}_{03};E)[\mathbb{S}_{RR;n'n}(\mathbf{q}_1,\mathbf{q}_{03};E)]^\dagger \\ &\times\mathbb{S}_{RL;n'm}(\mathbf{q}_1,\mathbf{q}_{01};E)\,\eta_{\rm env}(\mathbf{q}_{01},\mathbf{q}'_{01}).\end{aligned} \tag{A17}$$

[1] E. Joos, H. D. Zeh, C. Kiefer, D. Giulini, J. Kupsch, and I.-O. Stamatescu, *Decoherence and the Appearance of a Classical World in Quantum Theory* (Springer, Berlin, 2003).

[2] A. D. Stone, in *Physics of Nanostructures*, edited by J. H. Davies and A. R. Long (Institute of Physics and Physical Society, London, 1992).

[3] E. Akkermans and G. Montambaux, *Mesoscopic Physics of Electrons and Photons* (Cambridge University Press, Cambridge, 2007).

[4] Y. Imry, *Introduction to Mesoscopic Physics*, 2nd ed. (Oxford University Press, New York, 2002).

[5] A. Stern, Y. Aharonov, and Y. Imry, Phys. Rev. A **41**, 3436 (1990).

[6] G. Seelig, S. Pilgram, A. N. Jordan, and M. Büttiker, Phys. Rev. B **68**, 161310(R) (2003).

[7] Ph. Jacquod, Phys. Rev. E **72**, 056203 (2005).

[8] B. L. Altshuler, A. G. Aronov, and D. Khmelnitsky, J. Phys. C **15**, 7367 (1982); B. L. Altshuler and A. G. Aronov, in *Electron-Electron Interactions in Disordered Systems*, edited by A. L. Efros and M. Pollak (North-Holland, Amsterdam, 1985).

[9] S. Chakravarty and A. Schmid, Phys. Rep. **140**, 195 (1986).

[10] H. U. Baranger and P. A. Mello, Waves Random Media **9**, 105 (1999).

[11] P. W. Brouwer and C. W. J. Beenakker, Phys. Rev. B **55**, 4695 (1997); **66**, 209901(E) (2002).

[12] I. L. Aleiner, B. L. Altshuler, and M. E. Gershenson, Waves Random Media **9**, 201 (1999).

[13] H. Fukuyama and E. Abrahams, Phys. Rev. B **27**, 5976 (1983).

[14] I. L. Aleiner and A. I. Larkin, Phys. Rev. B **54**, 14423 (1996).
[15] B. N. Narozhny, G. Zala, and I. L. Aleiner, Phys. Rev. B **65**, 180202(R) (2002).
[16] M. Büttiker, Phys. Rev. B **33**, 3020 (1986).
[17] M. J. M. de Jong and C. W. J. Beenakker, Physica A **230**, 219 (1996).
[18] M. G. Vavilov and I. L. Aleiner, Phys. Rev. B **60**, R16311 (1999).
[19] G. Seelig and M. Büttiker, Phys. Rev. B **64**, 245313 (2001).
[20] M. L. Polianski and P. W. Brouwer, J. Phys. A **36**, 3215 (2003).
[21] C. Texier and G. Montambaux, Phys. Rev. B **72**, 115327 (2005).
[22] U. Eckern and P. Schwab, J. Low Temp. Phys. **126**, 1291 (2002).
[23] J. Tworzydlo, A. Tajic, H. Schomerus, P. W. Brouwer, and C. W. J. Beenakker, Phys. Rev. Lett. **93**, 186806 (2004).
[24] A. Altland, P. W. Brouwer, and C. Tian, Phys. Rev. Lett. **99**, 036804 (2007).
[25] C. Petitjean, P. Jacquod, and R. S. Whitney, JETP Lett. **86**, 736 (2007).
[26] A. G. Huibers, M. Switkes, C. M. Marcus, K. Campman, and A. C. Gossard, Phys. Rev. Lett. **81**, 200 (1998).
[27] A. G. Huibers, J. A. Folk, S. R. Patel, C. M. Marcus, C. I. Duruöz, and J. S. Harris, Phys. Rev. Lett. **83**, 5090 (1999).
[28] E. Buks, R. Schuster, M. Heiblum, D. Mahalu, and V. Umansky, Nature (London) **391**, 871 (1998).
[29] O. Yevtushenko, G. Lütjering, D. Weiss, and K. Richter, Phys. Rev. Lett. **84**, 542 (2000).
[30] A. E. Hansen, A. Kristensen, S. Pedersen, C. B. Sørensen, and P. E. Lindelof, Phys. Rev. B **64**, 045327 (2001).
[31] K. Kobayashi, H. Aikawa, S. Katsumoto, and Y. Iye, J. Phys. Soc. Jpn. **71**, 2094 (2002).
[32] F. Pierre, A. B. Gougam, A. Anthore, H. Pothier, D. Esteve, and N. O. Birge, Phys. Rev. B **68**, 085413 (2003).
[33] W. G. van der Wiel, Yu. V. Nazarov, S. De Franceschi, T. Fujisawa, J. M. Elzerman, E. W. G. M. Huizeling, S. Tarucha, and L. P. Kouwenhoven, Phys. Rev. B **67**, 033307 (2003).
[34] Strictly speaking, dephasing- and voltage-probe models are fully equivalent in the one channel limit only; however, they also lead to the same results in the limit of low temperature and frequency. See H. Förster, P. Samuelsson, S. Pilgram, and M. Büttiker, Phys. Rev. B **75**, 035340 (2007).
[35] C. W. J. Beenakker, Rev. Mod. Phys. **69**, 731 (1997).
[36] O. Bohigas, M. J. Giannoni, and C. Schmit, Phys. Rev. Lett. **52**, 1 (1984).
[37] M. L. Mehta, *Random Matrices* (Academic, New York, 1991).
[38] T. Guhr, A. Müller-Groeling, and H. A. Weidenmüller, Phys. Rep. **299**, 189 (1998).
[39] C. H. Lewenkopf and H. A. Weidenmüller, Ann. Phys. (N.Y.) **212**, 53 (1991); P. W. Brouwer, Phys. Rev. B **51**, 16878 (1995).
[40] S. Heusler, S. Müller, P. Braun, and F. Haake, Phys. Rev. Lett. **96**, 066804 (2006).
[41] M. G. Vavilov and A. I. Larkin, Phys. Rev. B **67**, 115335 (2003).
[42] H. Schomerus and Ph. Jacquod, J. Phys. A **38**, 10663 (2005).
[43] İ. Adagideli, Phys. Rev. B **68**, 233308 (2003).
[44] S. Rahav and P. W. Brouwer, Phys. Rev. B **73**, 035324 (2006).
[45] Ph. Jacquod and R. S. Whitney, Phys. Rev. B **73**, 195115 (2006).
[46] S. Rahav and P. W. Brouwer, Phys. Rev. Lett. **96**, 196804 (2006).
[47] O. Agam, I. L. Aleiner, and A. I. Larkin, Phys. Rev. Lett. **85**, 3153 (2000).
[48] J. Tworzydlo, A. Tajic, H. Schomerus, and C. W. J. Beenakker, Phys. Rev. B **68**, 115313 (2003).
[49] R. S. Whitney and Ph. Jacquod, Phys. Rev. Lett. **94**, 116801 (2005).
[50] R. S. Whitney and Ph. Jacquod, Phys. Rev. Lett. **96**, 206804 (2006).
[51] Ph. Jacquod and E. V. Sukhorukov, Phys. Rev. Lett. **92**, 116801 (2004).
[52] J. Tworzydlo, A. Tajic, and C. W. J. Beenakker, Phys. Rev. B **69**, 165318 (2004).
[53] P. W. Brouwer and S. Rahav, Phys. Rev. B **74**, 075322 (2006).
[54] At finite τ_E, the ergodic hypothesis breaks down and sample-to-sample conductance fluctuations are dominated by classical effects. They lose their universality and increase by orders of magnitude as τ_E/τ_D becomes sizable (see Refs. 51 and 52).
[55] K. Richter and M. Sieber, Phys. Rev. Lett. **89**, 206801 (2002).
[56] R. S. Whitney, Phys. Rev. B **75**, 235404 (2007).
[57] S. A. van Langen and M. Büttiker, Phys. Rev. B **56**, R1680 (1997).
[58] M. Büttiker, Phys. Rev. B **46**, 12485 (1992).
[59] W. H. Zurek, Rev. Mod. Phys. **75**, 715 (2003).
[60] W. G. van der Wiel, S. De Franceschi, J. M. Elzerman, T. Fujisawa, S. Tarucha, and L. P. Kouwenhoven, Rev. Mod. Phys. **75**, 1 (2003).
[61] F. Hofmann, T. Heinzel, D. A. Wharam, J. P. Kotthaus, G. Böhm, W. Klein, G. Tränkle, and G. Weimann, Phys. Rev. B **51**, 13872(R) (1995).
[62] A. S. Adourian, C. Livermore, and R. M. Westervelt, Appl. Phys. Lett. **75**, 424 (1999).
[63] D. S. Fisher and P. A. Lee, Phys. Rev. B **23**, R6851 (1981).
[64] H. U. Baranger, R. A. Jalabert, and A. D. Stone, Chaos **3**, 665 (1993).
[65] K. Richter, *Semiclassical Theory of Mesoscopic Quantum Systems*, Springer Tracts in Modern Physics, Vol. 161 (Springer, Berlin, 2000).
[66] Ph. Jacquod, Phys. Rev. Lett. **92**, 150403 (2004).
[67] C. Petitjean and Ph. Jacquod, Phys. Rev. Lett. **97**, 194103 (2006).
[68] M. C. Gutzwiller, *Chaos in Classical and Quantum Mechanics* (Springer, New York, 1991); J. Math. Phys. **12**, 343 (1971).
[69] F. Haake, *Quantum Signatures of Chaos*, 2nd ed. (Springer, Berlin, 2001).
[70] M. Sieber and K. Richter, Phys. Scr., T **T90**, 128 (2001); M. Sieber, J. Phys. A **35**, L613 (2002).
[71] More precisely, the encounter introduces a typical length scale $\delta r_\perp$ that corresponds to the perpendicular distance between the two paths in the vicinity of the encounter. Assuming hyperbolic dynamics, we get $\delta r_\perp = \frac{v_F \epsilon}{2\lambda} \sim L\epsilon$, and the exact definition of a typical cutoff time is given by $T_\ell(\epsilon) = \lambda^{-1} \ln[(\ell/\delta r_\perp)^2]$, with $\ell = \{L, W, \xi\}$.
[72] P. Collet and J.-P. Eckmann, J. Stat. Phys. **115**, 217 (2004).
[73] G. Berkolaiko, H. Schanz, and R. S. Whitney, Phys. Rev. Lett. **88**, 104101 (2002).
[74] M. W. Hirsch and S. Smale, *Differential Equations, Dynamical Systems, and Linear Algebra* (Academic, New York, 1974).
[75] P. Braun, S. Heusler, S. Müller, and F. Haake, J. Phys. A **39**, L159 (2006).
[76] This was not the case in Ref. 50 where we used the time independence of the problem to shift paths $\gamma 2$, $\gamma 3$ in time, so that all paths entered the cavity at the same time. Such a shift is unhelpful when the environment is present, so we do not do it here.
[77] R. P. Feynman and A. R. Hibbs, *Quantum Mechanics and Path Integrals* (McGraw-Hill, New York, 1965).
[78] For $\delta r_\perp \ll \lambda_F$, we evaluate the integral by approximating $e^{ix} \simeq 1$. For $\lambda_F \ll \delta r_\perp \ll L_\omega$, we split the integral into two at an arbitrary

value x', where $(\delta r_\perp / L_\omega) \ll x' \ll 1$. For the integral from $\delta r_\perp / L$ to x', we approximate $e^{ix} \simeq 1$, while for the integral from x' to $p_F \delta r_\perp / \hbar$, we approximate the denominator by x. In the latter case, we get an exponential integral, $Ei(z)$, whose properties at $z \ll 1$ and $z \gg 1$ are well known. The arbitrary cutoff, x', drops out of the final result, as it should. Finally, for $L_\omega \ll \delta r_\perp \sim L$, we can use integration by parts to perform an asymptotic expansion for large $\delta r_\perp / L_\omega$.

[79] Ph. Jacquod, H. Schomerus, and C. W. J. Beenakker, Phys. Rev. Lett. **90**, 207004 (2003).

[80] This has been first discussed in P. G. Silvestrov, J. Tworzydlo, and C. W. J. Beenakker, Phys. Rev. E **67**, 025204(R) (2003). For instance, numerical investigations of dynamical echoes observe a λ_{eff} that is smaller than $\lambda = \ln K/2$ because $\langle \exp[-\lambda t] \rangle \neq \exp[-\langle \lambda \rangle t]$, see, e.g., C. Petitjean, D. V. Bevilaqua, E. J. Heller, and Ph. Jacquod, Phys. Rev. Lett. **98**, 164101 (2007).

[81] Y. V. Fyodorov and H.-J. Sommers, JETP Lett. **72**, 422 (2000).

[82] J. H. Bardarson, J. Tworzydlo, and C. W. J. Beenakker, Phys. Rev. B **72**, 235305 (2005).

[83] Ya. M. Blanter and M. Büttiker, Phys. Rep. **336**, 1 (2000).